

See discussions, stats, and author profiles for this publication at: <https://www.researchgate.net/publication/269107188>

ChemInform Abstract: Aspartic Protease Inhibitors Containing Tertiary Alcohol Transition-State Mimics

ARTICLE in EUROPEAN JOURNAL OF MEDICINAL CHEMISTRY · NOVEMBER 2014

Impact Factor: 3.45 · DOI: 10.1016/j.ejmech.2014.11.036

CITATIONS

2

READS

157

5 AUTHORS, INCLUDING:



Hitesh V Motwani

Stockholm University

20 PUBLICATIONS 28 CITATIONS

[SEE PROFILE](#)



Maria De Rosa

Uppsala University

9 PUBLICATIONS 91 CITATIONS

[SEE PROFILE](#)



Luke R. Odell

Uppsala University

61 PUBLICATIONS 659 CITATIONS

[SEE PROFILE](#)



Mats Larhed

Uppsala University

234 PUBLICATIONS 6,171 CITATIONS

[SEE PROFILE](#)



Invited review

Aspartic protease inhibitors containing tertiary alcohol transition-state mimics



Hitesh V. Motwani, Maria De Rosa, Luke R. Odell, Anders Hallberg, Mats Larhed*

Department of Medicinal Chemistry, Organic Pharmaceutical Chemistry, BMC, Uppsala University, P.O. Box 574, SE-751 23 Uppsala, Sweden

ARTICLE INFO

Article history:

Received 9 September 2014

Received in revised form

12 November 2014

Accepted 19 November 2014

Available online 20 November 2014

Keywords:

Protease inhibitors

Tertiary alcohol

Transition-state mimic

HIV

Malaria

Alzheimer

ABSTRACT

Aspartic proteases (APs) are a class of enzymes engaged in the proteolytic digestion of peptide substrates. APs play important roles in physiological and infectious pathways, making them plausible drug targets. For instance in the treatment of HIV infections, access to an efficient combination of protease and reverse transcriptase inhibitors have changed a terminal illness to a chronic but manageable disease. However, the benefits have been limited due to the emergence of drug resistant viral strains, poor pharmacokinetic properties of peptidomimetic inhibitors and adverse effects associated with the treatment. In the 1980s, D. Rich and co-workers proposed a novel strategy for the development of AP inhibitors by replacing the secondary hydroxyl group with a tertiary alcohol as part of the transition state (TS) mimicking moiety. This strategy has been extensively explored over the last decade with a common belief that masking of the polar group, e.g. by intramolecular hydrogen bonding, has the potential to enhance transcellular transport. This is the first review presenting the advances of AP inhibitors comprising a tertiary hydroxyl group. The inhibitors have been classified into different *tert*-hydroxy TS mimics and their design strategies, synthesis, biological activities, structure–activity–relationships and X-ray structures are discussed.

© 2014 Elsevier Masson SAS. All rights reserved.

1. Introduction

1.1. Aspartic proteases: mechanism of action, relevance in the field of drug discovery and development of transition state mimicking inhibitors

Proteases are a family of enzymes that catalyze the hydrolysis of peptide bonds in proteins and polypeptides, a reaction that is vital to both physiological and pathological processes. The human genome encodes over 500 proteases (MEROPS database), making this group one of the largest enzyme families. Proteases are commonly classified into six classes: serine, threonine, cysteine,

glutamic, metallo and aspartic proteases (APs) [1–3]. APs are the smallest class in the human genome with only 15 members, but they have long been a rich source of potential drug molecules in the field of drug discovery [4]. The APs have been classified into two clans: clan AA and clan AD, based on their tertiary structures. Clan AA consists of two families: family A1, which contains the classical aspartic proteases (renin, pepsin A, pepsin C, cathepsin D, cathepsin E, BACE-1, BACE-2 and napsin A) and family A2, which contains proteases such as HIV-1 protease that can be integrated into the human genome by retroviruses. Clan AD comprises of presenilins and signal peptide peptidase, which are the intra-membrane cleaving proteases [1–3].

APs use an aspartic acid (Asp) dyad to hydrolyze peptide bonds. Most APs bind to 6–10 amino acid residues in the substrate, which can then be used to design substrate-based inhibitors. APs also have one or more flaps in their structure that close down to cover the substrate/inhibitor, resulting in further interactions within the complex. For example, in the case of the dimeric AP HIV-1 protease, it is thought that a water molecule in the active site is activated by a deprotonated aspartic acid (Asp25 or Asp125), which facilitates a nucleophilic addition to the amide carbonyl carbon in the substrate to form a tetrahedral intermediate compound [the transition state (TS) [5]; Fig. 1]. The other aspartic acid can donate a proton to the

Abbreviations: AIDS, acquired immune deficiency syndrome; AD, Alzheimer's disease; $\text{A}\beta$, amyloid beta; AP, aspartic protease; Asp, aspartic acid; C_{int} , intrinsic clearance; CC_{50} , 50% of the cytotoxic concentration; EC_{50} , half the maximum effective concentration; HIV, human immunodeficiency virus; IC_{50} , concentration required to inhibit enzyme activity by 50%; K_i , inhibition constant; Me^3Sta , 4-amino-3-hydroxy-3,6-dimethylheptanoic acid; P_{app} , permeability; PDB, protein data bank; PI, protease inhibitor; SAR, structure–activity–relationship; TBS, *tert*-butyldimethylsilyl; TS, transition state; WHO, World Health Organization.

* Corresponding author.

E-mail address: Mats.Larhed@orgfarm.uu.se (M. Larhed).

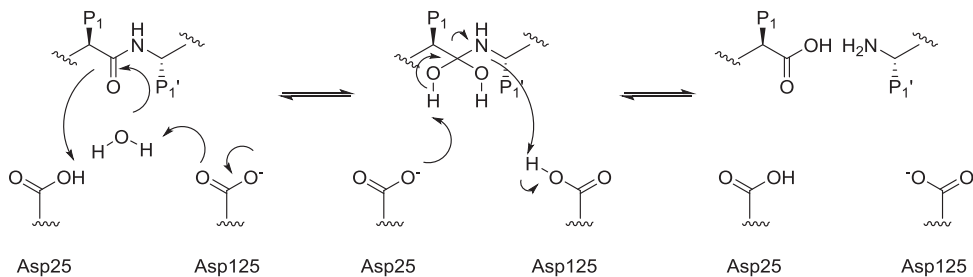


Fig. 1. The mechanism of peptide bond cleavage by an AP, as exemplified by HIV-1 protease. Since HIV-1 protease is a dimeric C-2 symmetric AP, the active aspartic acids are denoted Asp25 and Asp125.

nitrogen in the amide bond and the TS thus separates into two products: an acid fragment (the N-terminal product) and an amine fragment (the C-terminal product) [6,7]. A detailed description of the proteases molecular structures is beyond the scope of this review and have been reviewed elsewhere [2,3,8].

Following standard nomenclature, the amino acids on the C-terminal side of the scissile bond are denoted $P_1'-P_2'-P_3'\dots-P_n'$, while those on the N-terminal side are denoted $P_1-P_2-P_3\dots-P_n$. The corresponding pockets in the enzyme are denoted $S_1'-S_2'-S_3'\dots-S_n'$ and $S_1-S_2-S_3\dots-S_n$ on the C-terminal and N-terminal sides of the scissile bond, respectively (Fig. 2) [9]. The crystal structures of most of the A1 human APs have been solved [10–15]; some of them are presented in later sections of this review as X-ray crystallography depictions of enzyme–inhibitor complexes.

There are a number of factors that should be considered when developing protease inhibitors (PIs) as oral therapeutic drugs. The ideal PI should be very potent and highly selective for the specific protease, with appropriate pharmacokinetic and pharmacodynamic characteristics. Because peptides are usually associated with low bioavailability and short half-lives, the candidates should be minimally peptidic in nature. Further, to be potential pharmaceutical compounds, they should have low toxicity, a high therapeutic index, high membrane permeation characteristics, good oral bioavailability and a clearance rate that will allow administration of only one or two doses a day. Strategies for discovering PIs include natural product screening, mimicking the natural peptide substrate and replacing the scissile amide bond with a non-cleavable isostere and computer-assisted substrate-based design using information on the structure of the substrate or inhibitor–enzyme complex obtained by nuclear magnetic resonance (NMR) spectroscopy and/or X-ray crystallography.

The investigations into the use of APs as drug targets were pioneered with the development of renin and HIV-1 PIs [3,16,17]. Substrate-based inhibitors, which mimicked the TS in the peptide cleavage process but contained a non-cleavable isostere in place of the scissile amide bond, were developed in these early strategies [3,16]. Pepstatin A (Iva-Val-Val-Sta-Ala-Sta), first isolated by Umezawa et al. [18], is a naturally occurring inhibitor of APs that has been used as a model compound in this respect. Pepstatin A contains the amino acid statine [(3S,4S)-4-amino-3-hydroxy-6-methylheptanoic acid; Sta] as a putative TS mimic and is active against most APs with inhibition constant (K_i) values in the range of 0.1–1 nM. Synthetic manipulations of the pepstatin structure have led to the discovery of novel, potent renin and other AP inhibitors.

The AP renin plays an important physiological role in the regulation of blood pressure. It controls the first (rate-limiting) enzymatic step in the renin-angiotensin system (RAS) by catalyzing the cleavage of the Leu10–Val11 peptide bond in angiotensinogen, to release the decapeptide angiotensin I. Renin is an essential and specific enzyme and angiotensinogen is its only known physiological substrate [19,20]. Despite the fact that the first renin

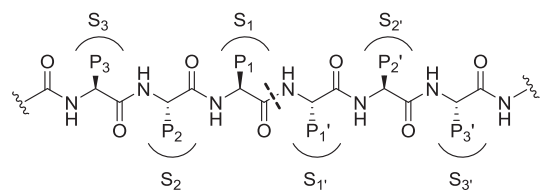


Fig. 2. The nomenclature commonly used to describe amino acid moieties and the corresponding enzyme pockets of APs. The scissile bond is denoted by a dashed line.

inhibitor, Aliskiren, was only approved in 2007 [21], the results of research efforts in this area over the past 30 years have proven invaluable when targeting other APs such as HIV-1 protease. Although no tertiary alcohol renin inhibitors have been reported to date, we decided to briefly include them in this review because the first APs to be targeted for drug development, pioneered by Daniel Rich in the early 1980s, were the renin inhibitors [22,23]. Fig. 3 shows examples of various potent secondary alcohol-based renin inhibitors. The concept of replacing the scissile peptide bond by non-cleavable isosteres in the TS intermediate was introduced by Szelke et al. [24] as a result of the early research into renin inhibitors. This strategy has since become so successful that it has become the primary method of designing AP inhibitors [3,25,26].

Most of the AP inhibitors available on the market today (excluding tipranavir) possess peptidomimetic characteristics with a non-hydrolyzable bond replacing the scissile bond. The most commonly used TS mimic, as seen in the HIV-1 PIs, is the hydroxyethylene moiety [17]. However, many other TS mimics have been successfully tested as AP inhibitors and these are exemplified in Fig. 4. These sec-hydroxy TS mimics have been reviewed extensively in the literature, for example by Leung et al. [25] and Cooper [26].

Our group has been engaged in the development of novel HIV-1 PIs since the mid 1990s [27–46]. Inspired by the work of Lam et al. [47], we initially targeted symmetric and asymmetric cyclic HIV-1 PIs [48–51]. Following the approval of linear HIV-1 PIs by the FDA in 1995, the focus moved to linear inhibitors. Structural fragments that seemed potentially interesting were obtained from molecules such as indinavir, launched in 1996 and atazanavir, launched in 2003 (Fig. 5). Interestingly, atazanavir was the first PI to be recommended for once-daily administration, thus reducing the tablet burden for the patient. The prediction of binding affinities/energies and selectivity obtained from computational molecular dynamics simulations [52,53] and free-energy perturbation simulations [54], most of which were conducted by Johan Åqvist's team in the early 2000s, was an important contribution to the development of AP inhibitors.

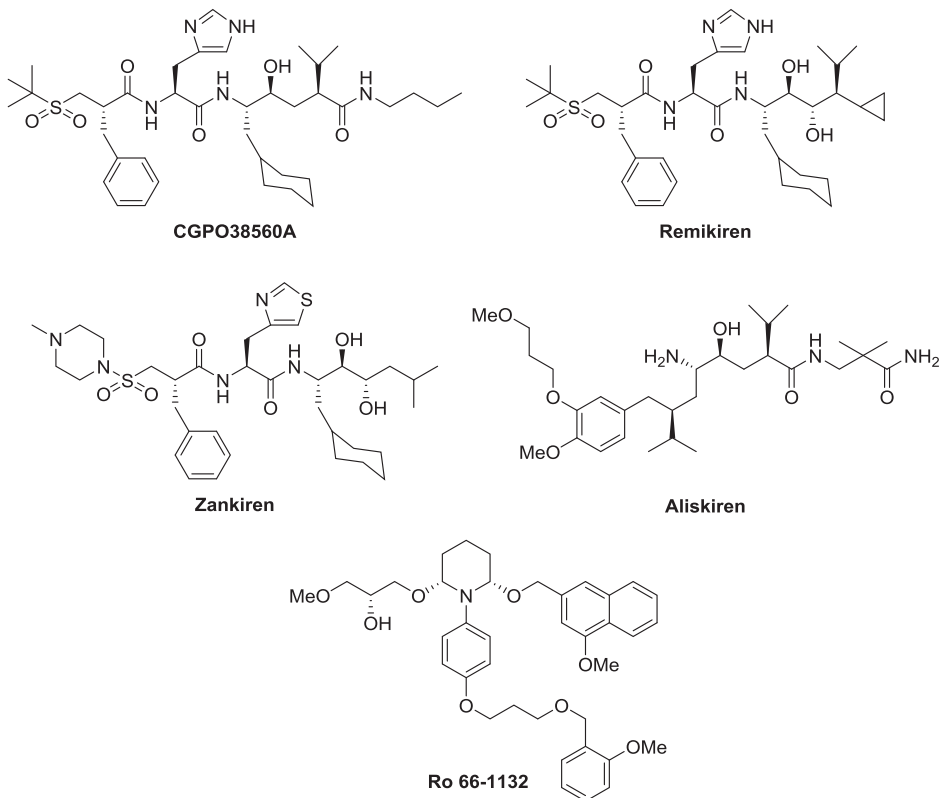


Fig. 3. Renin inhibitors containing sec-hydroxy TS mimics. Tetrapeptide TS mimetic inhibitors CGPO38560A [concentration required to inhibit enzyme activity by 50% (IC_{50}) 1 nM], remikiren (IC_{50} 0.7 nM) and zankiren (IC_{50} 1.1 nM); the non-peptidomimetic inhibitor aliskiren (IC_{50} 0.6 nM); and the 3,4,5 substituted piperidine Ro 66-1132 (IC_{50} 0.07 nM). Remikiren and zankiren contain dihydroxy isosteres.

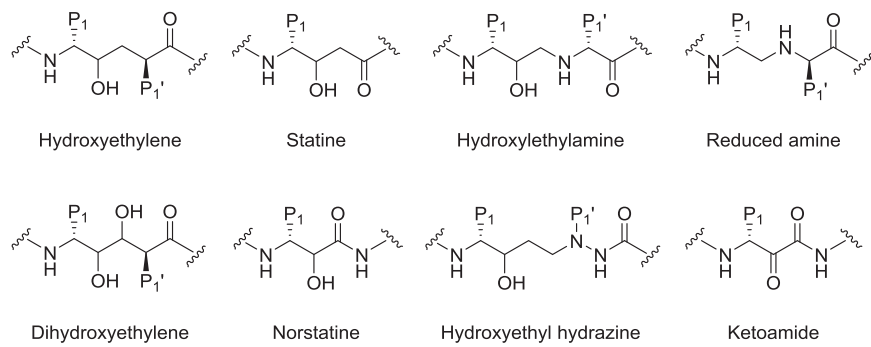


Fig. 4. Examples of sec-hydroxy (and ketone-containing) TS mimics.

1.2. Tert-hydroxy transition-state mimics: overview and classification

In order to act as potent antivirals, AP inhibitors must be able to pass across the lipid bilayer of epithelial cell membranes. Although lipophilicity is often used as a molecular descriptor to predict the passive diffusion of molecules through membranes, this descriptor does not correlate well with the membrane permeation properties of small peptides across Caco-2 cell monolayers. An alternative property, which does correlate with membrane permeation characteristics, is the hydrogen bonding potential [55,56]. The desolvation energy needed for a compound to enter into the lipophilic membrane phase from the aqueous phase is decreased in compounds with intramolecular hydrogen bonds because of the reduced hydrogen bonding potential. This correlation between the

masking of polar groups and enhanced membrane permeation has been described in several reports [57–60]. Most of the early therapeutically useful AP inhibitors contain a polar secondary alcohol in the analog unit mimicking the TS. Thus, enhanced membrane permeation is obtained by masking the crucial hydroxyl group in these compounds via internal hydrogen bonding in the appropriate chemical environment.

In general, a TS mimic containing a *tert*-alcohol can be created by relocating the “central” secondary hydroxyl group in the analogs, e.g. hydroxyl ethylene, statine and hydroxylethylamine (Fig. 4). The reason for this relocation is to mask the hydroxyl unit and this can be obtained by, for example, increasing internal hydrogen bonding, which will subsequently enhance transcellular transport, a step towards achieving improved oral bioavailability. The enhancement of membrane permeation by masking polar groups

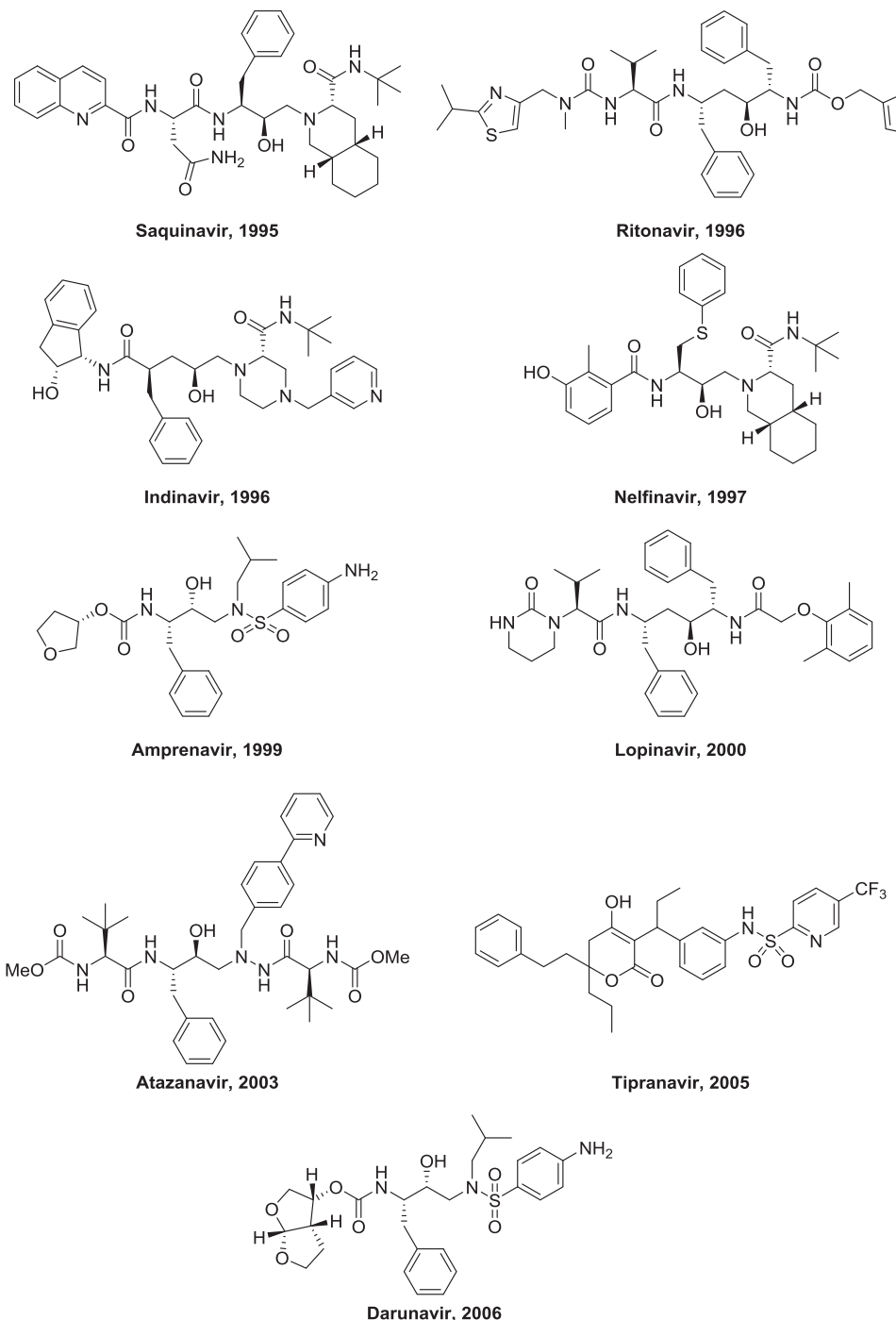
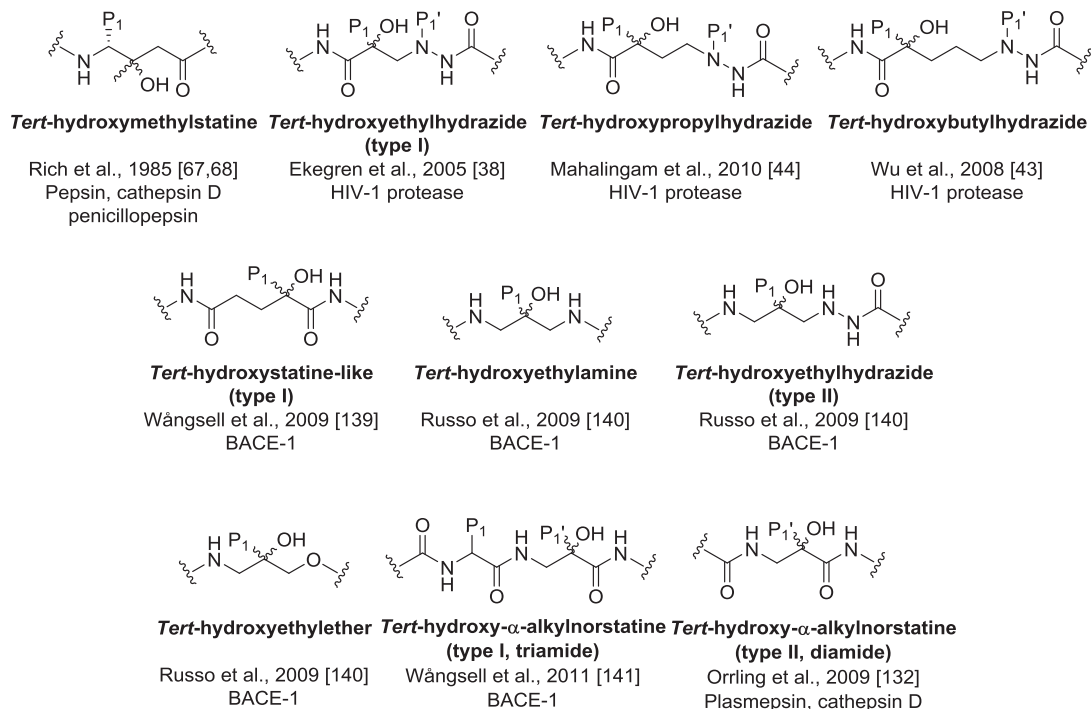


Fig. 5. FDA-approved HIV-1 PIs containing sec-hydroxy TS mimics.

has been effectively used in various scenarios. It was through the combination of this idea with preliminary modeling and several years' experience with sec-OH-containing inhibitors that our focus was shifted to developing HIV-1 PIs with the novel tertiary-hydroxyethyl hydrazide as a TS mimic (refer Section 3 for more details). The first HIV-1 PI scaffold with a tertiary alcohol TS mimic was presented from our group by Ekegren et al. in 2005; this compound had a one-carbon spacer between the tertiary alcohol and the hydrazide group [38].

Fig. 6 provides a classification of AP inhibitors containing a tertiary alcohol TS mimic, found in the literature. In the following

sections we provide a detailed view of these AP inhibitors, based on chemistry, biological evaluation and X-ray crystallography. Because there are many of such inhibitors in the literature, we focus mainly on those with a K_i value <10 nM. While many tertiary alcohol inhibitors with a K_i value >10 nM are presented in the literature, only a few of these are included in this review, when considered necessary for structure–activity-relationship (SAR) comparisons.

Fig. 6. General classification of AP inhibitors containing *tert*-hydroxy TS mimics.

2. Pepsin, cathepsin D and penicillopepsin inhibitors

2.1. Background

Pepsin is a digestive protease enzyme whose zymogen (pepsinogen) is released in the stomach; the conversion of the zymogen to the enzyme is based on the removal of the N-terminal region consisting of about 40 residues [61]. Pepsin was discovered in 1836 by Theodor Schwann and was amongst the first enzymes to be crystallized (by John Northrop in 1929). Pepstatin, a low molecular weight compound, is a potent inhibitor specific for acid proteases with a K_i of ca. 1 nM for pepsin. The statyl residue of pepstatin is responsible for the inhibition of pepsin; statine is an analog of the TS for catalysis by pepsin and other acid proteases. Cathepsin D is a major endopeptidase that is present in lysosomes [3,61]. It has a broad peptide bond specificity that is similar to that of pepsin; however, unlike the gastric protease, cathepsin D functions inside the cell. Estrogens in breast cancer cells are believed to regulate the expression of this AP by a non-consensual estrogen-response element [62]. The pathogenesis of several diseases, including breast cancer and Alzheimer's disease (AD), could possibly result from mutations in the CSTD gene that encodes the cathepsin D protein. Penicillopepsin can be described as a fungal AP that possesses trypsinogen-activating properties [63,64]. Peptides such as Ac-Ala-Ala-Lys-Phe(NO₂)-Ala-Ala-NH₂, which is a good substrate for fungal APs, can be cleaved between the lysine and *p*-nitrophenylalanine residues by penicillopepsin at a faster rate than achieved by human renin. The fungal APs are homologous to pepsin and show similarities in their specificity for mammalian enzymes; however, most small pepsin substrates are not hydrolyzed by penicillopepsin [65,66].

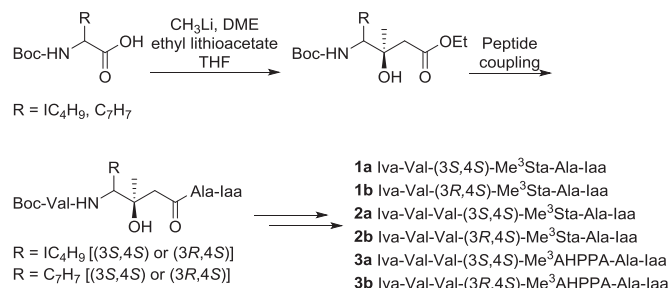
2.2. *Tert*-hydroxymethylstatine

In 1985, Rich et al. reported a series of modified pepstatin analogs in which statine was replaced by 4-amino-3-hydroxy-3,6-

dimethylheptanoic acid (Me³Sta) or 4-amino-3-hydroxy-3-methyl-5-phenylpentanoic acid (Me³AHPPA) [67,68]. The 3S,4S and 3R,4S diastereomers of each analog were tested for inhibition potency against pepsin, cathepsin D and penicillopepsin.

Fig. 7 shows the route for synthesizing Me³Sta and Me³AHPPA derivatives **1–3** [67,69]. The chirality of the diastereomers was determined by forming oxazolidinone derivatives from the free amino acid available as a mixture of diastereomers. The oxazolidinones were analyzed by ¹³C and NOE NMR experiments, which

Synthesis of Me³Sta and Me³AHPPA derivatives



Biological data of selected inhibitors

Cmpd	Structure	<u>K_i (nM)</u>		
		pepsin	cathepsin D	penicillopepsin
1b	Iva-Val-(3R,4S)-Me ³ Sta-Ala-Iaa	100		
2b	Iva-Val-Val-(3R,4S)-Me ³ Sta-Ala-Iaa	1.5	214	80
3b	Iva-Val-Val-(3R,4S)-Me ³ AHPPA-Ala-Iaa	2.1		12

Fig. 7. Chemistry and biological evaluation of the *tert*-hydroxymethylstatine TS-mimicking inhibitors. Empty spaces indicate data that are not available.

showed that the main product for both the Me³Sta and Me³AHPPA analogs was the 3S,4S-diastereomer. The diastereomeric amino acid mixture was bound to L-Ala-Iaa and the subsequent diastereomeric dipeptides were separated using column chromatography and were then used to form the desired final inhibitors (Fig. 7) [67,69]. Fig. 7 also shows the *K_i* values for *tert*-hydroxy compounds **1b**, **2b** and **3b**. One peptide (3R,4S) from each diastereomeric pair was 2–3 orders of magnitude more potent as an inhibitor of the AP (whether pepsin, penicillopepsin or cathepsin) than the other (3S,4S). Increasing the length of the peptide chain generally resulted in more potent inhibitors and the difference between the *K_i* values for the respective diastereomers also increased. This is exemplified by comparing **1b** with **2b**; when the peptide chain was lengthened by one residue, the inhibition constant for pepsin was decreased by a factor of nearly 100.

The inhibitors were more potent against pepsin than against cathepsin D. However, when the iso-butyl side chain in Sta was replaced by a benzyl group to form AHPPA analogs, the inhibition activity against cathepsin D was increased in contrast to that against pepsin. Inhibitor **3b**, a Me³AHPPA derivative, was ca. 20 times more active than the corresponding Me³Sta derivative **2b**.

In summary, it was observed that in all AP inhibition tests the 3R,4S diastereomers of both the Me³Sta and Me³AHPPA inhibitors were more potent than the corresponding 3S,4S diastereomers. The *K_i* values of the best inhibitors were in the range 1.5–12 nM. Interestingly, these results were in contrast to those obtained for the *sec*-OH-based inhibitors containing statine or AHPPA derivatives, in which the 3S,4S diastereomer was the more potent inhibitor for each of the diastereomeric pairs of derivatives. The statine- and AHPPA-based inhibitors were only ca. 10-fold more potent than the corresponding Me³Sta and Me³AHPPA inhibitors, which as expected were 100- to 1000-fold more potent than inhibitors without the C-3 OH group. Rich et al. also found that conformational changes in porcine pepsin were induced by (3R,4S)-Me³Sta derivatives that were comparable to changes induced by pepstatin binding. These changes were not induced by the corresponding 3S,4S analog [68].

3. HIV-1 protease inhibitors

3.1. Background

The nucleotide sequence of the HIV genome, published in 1985 by Wain-Hobson et al. [70], revealed the coding sequences of 15 viral proteins, including the AP HIV-1 protease. HIV-1 protease consists of a two-fold symmetric dimer that possesses two identical subunits, each containing 99 amino acids. The HIV protease includes a conserved catalytic site, comprising the catalytic triad Asp25, Thr26 and Gly27 in each subunit, which is accountable for its activity [71,72]. The conformation of the dimers is changed, with loss of symmetry, by binding to natural asymmetric substrates or a PI. The relevant cleavage sites are located by the protease more by recognition of peptide shape than by the amino acid sequence. A precise order for the cleavages, with cleavage rates specific for each site, is generated by small variations amongst the different cleavage loci. As the active form of the HIV-1 protease is a dimer, it has been suggested that the activity of the protease is influenced by the concentrations of its subunits [71,72]. The degradation of viral proteins prior to the budding of new viral particles is thus prevented. As soon as the role of the protease was elucidated in the viral replication cycle, it was identified as a possible drug target. Gag and Gag-Pol polyproteins are processed by HIV-1 protease to form active proteins and enzymes together with the structural capsid proteins (MA, CA, NC) and the enzymes (PR, RT, IN), to make nine cleavage sites in total [73]. The general catalytic mechanism

for AP, as described in section 1.1 (Fig. 1), is believed to be followed for the peptide bond cleavage process by HIV-1 proteases.

X-ray analysis of HIV-1 protease co-crystallized with substrate-based inhibitors was first carried out in 1989 [71,74–76]. Two structural flaps, one from each monomer, cover the active site (Fig. 8). These flaps are flexible and can be in an open or closed position. The entry of substrates into the enzyme is easier when they are in the open position, while the processing of substrates is enhanced when they are in the closed position. The active site of the protease is bound competitively by the PI, and Ile50 and Ile150 (from monomers one and two, respectively) can incorporate a structural water molecule when the flaps are in the closed position.

Over the past 20–30 years, many structural and mechanistic insights have been gained by studying the HIV protease and this resulted in the establishment of several inhibitory principles. HIV-1 PIs were the first of the AP inhibitors to reach the market and they continue to serve as prototype inhibitors for the whole AP enzyme family. Nevertheless, nearly three decades after the discovery of AIDS, the pandemic of this viral disease is still on the rise; worldwide at the end of 2012 ca. 35 million people were living with the disease and 1.6 million people had died of AIDS-related illnesses in the same year [World Health Organization (WHO), Global Health Observatory]. Currently, there are 11 FDA-approved HIV PIs; saquinavir is now marketed as saquinavir mesylate and amprenavir has been replaced by its prodrug fosamprenavir (Fig. 5). Introduction of the HIV-1 PIs in the 1990s [77–80] had a large impact on HIV-infected patients, as seen by the substantial increase in survival rates and improved quality of life. However, the clinical benefits of this class of antiviral agents are restricted by a number of factors. Firstly, many of the marketed HIV-1 PIs, especially in the first generation, had poor pharmacokinetic properties, resulting in poor aqueous solubility, low metabolic stability, high protein binding and poor membrane permeation. This limitation meant that high doses were required to keep the viral plasma levels down and this subsequently resulted in poor patient compliance because of the severe side effects from the high doses. Some of the side effects caused by the PIs were gastrointestinal complications including nausea, vomiting and diarrhea, and metabolic disorders such as hyperlipidemia, lipodystrophy and insulin resistance [81,82]. However, many of the pharmacokinetic problems have been addressed by new contributions to the available arsenal of HIV-1 PIs, for instance the development of non-peptidomimetic inhibitors as possible therapeutic option [83], and the addition of low-dose ritonavir as a pharmacokinetic booster [84]. Another serious threat to efficient HIV treatment is the development of resistance to the marketed HIV-1 PIs [85,86]. This is a consequence

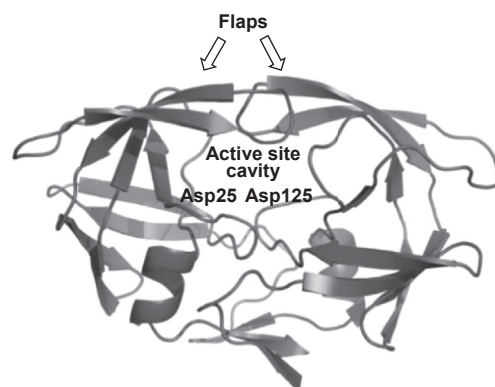


Fig. 8. The secondary structure of HIV-1 protease shown as a ribbon cartoon with the flaps closed on top and the active site as the central cavity (PDB code: 2xye).

of the high viral replication rate and the large number of errors that occur during the viral replication process. It is vitally important to combat this problem; this can be achieved by improving available pharmacotherapeutic options and developing new HIV-1 PIs, such as the *tert*-hydroxy class of compounds discussed in this review.

The HIV-1 PIs comprising *tert*-hydroxy TS mimics are classified here into three categories, with the common name *tert*-hydroxalkylhydrazide, where alkyl represents ethyl, *n*-propyl and *n*-butyl (Fig. 6). The chemistry, biological evaluation and X-ray crystallography of this class of inhibitors are discussed below.

3.2. *Tert*-hydroxyethylhydrazide (type I)

Preliminary modeling studies from our group indicated that a tertiary alcohol in the α -position to a carbonyl, linked with the ethylhydrazine group successfully used in atazanavir, could provide potent inhibitors. This led to the exploration of the *tert*-hydroxyethylhydrazide (type I) TS isostere, first published in 2005 [38], that is presented in this section [whereas *tert*-hydroxyethylhydrazide (type II) is reviewed later, in Section 5.3].

3.2.1. Variations in the P1'-P3' moiety

We started by investigating the decoration of the core structure with the (1*S*,2*R*)-1-amino-2-indanol P2 group, which is also present in indinavir, with benzyl P1 and P1' residues and amino-acid-derived P2'/P3' side chains (Fig. 9) [38].

Different procedures for preparing quaternary carbon centers, using various starting materials, can be found in the literature [87]. The procedure described here [38] is the one we used to synthesize chiral quaternary carbon atoms bearing the required tertiary alcohol by ring-opening reactions with 2,2-disubstituted epoxides (Fig. 10). The commercially available benzylmalonic acid **4** was used to synthesize the precursor of the inhibitor with P1 benzyl and P2 (1*S*,2*R*)-1-amino-2-indanol group, epoxide **8**, in three steps. A Mannich reaction of the malonic acid **4** with diethylamine and formaldehyde followed by *in situ* decarboxylation gave 2-benzylacrylic acid **5** [88]. Amide coupling of **5** with (1*S*,2*R*)-1-amino-2-indanol **6** provided the α,β -unsaturated amide **7**, which was epoxidized using *m*CPBA to give a mixture of diastereomers (*S*)-**8** and (*R*)-**8** (where *S* and *R* refer to the absolute configuration of the epoxide chiral center).

The hydrazide unit linkage between the P1' and P2' groups was obtained by coupling benzyl hydrazines **9** to L-valine **10a** or L-*tert*-leucine **10b**. Two different P1' side chains were prepared from benzylhydrazine **9a** and 4-bromo-benzylhydrazine **9b**. Finally, regioselective ring opening of epoxides (*S*)-**8** and (*R*)-**8** using hydrazides **11** gave the desired PIs **12** (Fig. 10).

The inhibitors were tested in an HIV-1 protease assay and evaluated for *in vitro* antiviral activity in HIV-1-infected MT4 cells, and the corresponding K_i and half the maximum effective

concentration (EC₅₀) values were determined (examples given in Fig. 10) [38]. The (*S*)-OH compounds such as **12b** (K_i 6.0 nM) were far more potent PIs (ca. 40× lower K_i values) than the corresponding (*R*)-configuration. A 2- to 4-fold increase in potency was seen for the *para*-bromo compound **12a** in comparison with the unsubstituted compounds **12b-c**. With regard to the *N*-substitution SAR, it was observed that the methoxycarbonyl derivatives **12a-c**, which had K_i values of 2.4–9.0 nM, were more potent than the benzyloxycarbonyl and benzylurea derivatives with K_i values of 17–23 nM, which could have resulted from unfavorable steric interactions. The compounds containing *N*-methoxycarbonyl P3' groups (**12a-c**) were the only examples of this series with any anti-HIV activity in the cell assay (MT4). With a *tert*-butyl P2' group **12b**, the EC₅₀ was 2-fold less than the corresponding *iso*-propyl compound **12c**, which is in accordance with results from the atazanavir series [89]. The most active compound in this class **12a** had a K_i value of 2.4 nM and an EC₅₀ value of 1.1 μ M.

When compounds **12a** and **12b** were tested *in vitro* with two ritonavir-resistant or a symmetric diol-based inhibitor-resistant HIV-1 strains [28], it was observed that their potencies against these mutant viruses and the wild type were similar (Fig. 10). High permeability was observed through the Caco-2 cell layers, with apparent permeability (P_{app}) values of 42×10^{-6} and 35×10^{-6} cm/s for compounds **12a** and **12b**, respectively. However, this is in contrast to the low cellular antiviral activities for these compounds. This might be because of the high protein binding of the inhibitors in the MT4 cell assay. In addition, inhibitors **12a** and **12b** had intrinsic clearance (Cl_{int}) values of 266 and 527 μ L/min/mg, respectively, suggesting that they might be rapidly degraded by metabolic enzymes, similar to compounds containing the (1*S*,2*R*)-1-amino-2-indanol group [90,91].

3.2.2. P1' extension

As discussed above (Section 3.2.1), compounds acquired after varying the P1'-P3' moiety were relatively potent enzyme inhibitors, but all of them possessed low antiviral activity in cell culture. Further, it was apparent from the **12a**-HIV-1 enzyme complex X-ray crystallography data (cf. Sections 3.2.5 and 3.3.5 below) that penetration of the P1' side chain in compound **12a** was not as deep into the S1' enzyme site as that in indinavir, suggesting that the enzyme pocket was not substantially occupied. As a result, an extension of the P1' position seemed suitable for optimization of the scaffold to increase the potency and cellular activity of the desired potential inhibitor [41].

A set of P1'-extended inhibitors was therefore prepared, starting from compound **12a**, the most active inhibitor from the first series (Fig. 10). Microwave-assisted Pd(0)-catalyzed cross-coupling reactions were performed on the *para*-bromo compound **12a** [41], where Pd(PPh₃)₂Cl₂ (5–10 mol%) was used as the pre-catalyst, with a maximum reaction time of 1 h [92–94]. The *meta*-substituted series was obtained using similar cross-coupling reactions on the *meta*-bromo analog **13** [41]. The general synthetic scheme for the synthesis of P1'-extended inhibitors and the biological inhibition data are shown in Fig. 11.

It was observed that the *para* P1'-extended compounds were in general more active, with K_i values 2.1–20 nM, than the *meta*-substituted compounds, which was probably due to the improved angle of approach by the *para*-substituted P1' side chains into the S1' pocket of the enzyme. The most active compound in the series was **14a**, with a K_i of 2.1 nM. The cellular antiviral activities appeared to be highly dependent on the substituent [41]. The relatively higher potency of these compounds, in comparison with those in Fig. 10, could be explained by their high lipophilicity arising from the large hydrophobic P1' side chains. The *para*-substituted bromo **12a**, 2-pyridyl **14d** and heterocyclic **14a** showed similar cell-

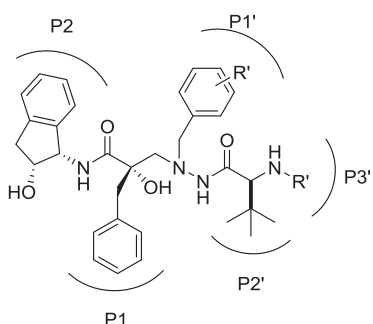


Fig. 9. General structure of the *tert*-hydroxyethylhydrazide (type I) class of HIV-1 PIs.

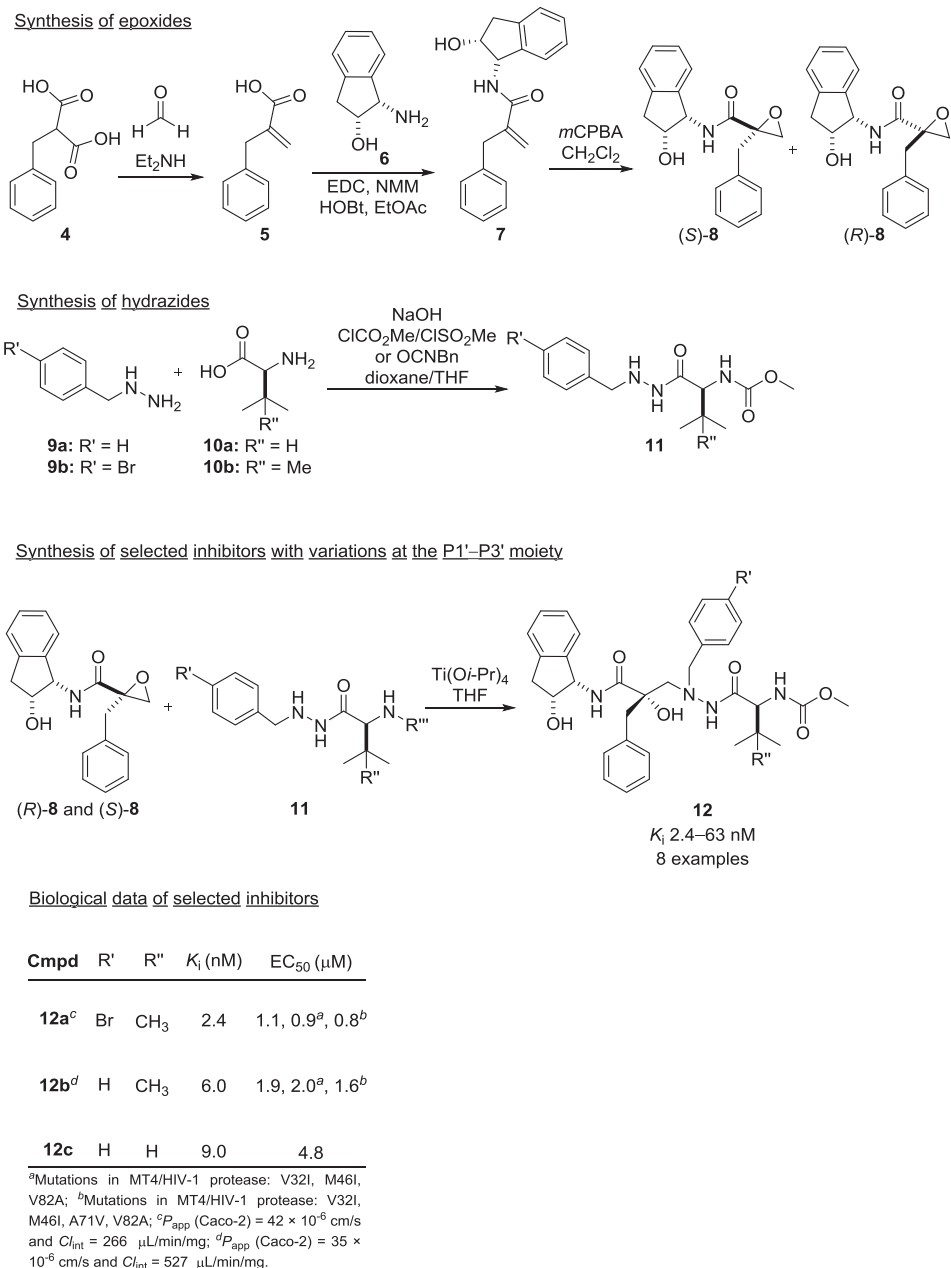


Fig. 10. Synthesis and biological evaluation of the *tert*-hydroxyethylhydrazide (type I) TS-mimicking HIV-1 PIs with variations in the P1'-P3' moiety.

based antiviral potency (EC₅₀ 0.90–1.1 μM), whereas 3-pyridyl **14c** was more potent (EC₅₀ 0.18 μM). Membrane permeation and liver microsome stability studies (Caco-2 assay) were conducted on the 3-pyridyl-extended compound **14c** and its *meta*-analog **15a** [41]. The P_{app} values were 33 × 10⁻⁶ and 11 × 10⁻⁶ cm/s, respectively, suggesting excellent permeation for the *para* compound **14c** in contrast to the *meta* compound [41]. The intrinsic clearance for both inhibitors was lower than that for the compounds in Fig. 10 (C_{int} 154 and 190 μL/min/mg, respectively).

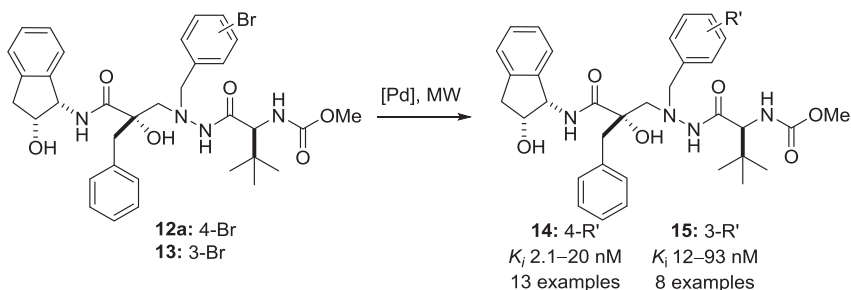
3.2.3. Variations in the P2 moiety

Although highly potent inhibitors were obtained from the P1' extended side chains (see above), the inhibitors were prone to rapid metabolism when evaluated with liver microsomes, as indicated by their intrinsic clearance values [41]. This may have been due to benzylic oxidation of the P2 group (1*S*,2*R*)-1-amino-2-indanol

[90,91], which led us to investigate variations in the P2 group [40]. Motivation for this study also came from considering the FDA-approved inhibitors saquinavir, nelfinavir and amprenavir, which have cyclic P2 substituents, whereas L-valine and L-*tert*-leucine are present as P2/P3 and P2'/P3' side chains in the atazanavir analog series. A set of compounds with varying P2 groups was thus prepared by coupling (S)-16 with various amides and opening the ring with a *para*-bromobenzylhydrazide **11**, as shown in Fig. 12 [40].

Compounds **17a** and **17b**, with amino-acid-derived iso-propyl P2 groups, showed high potency (K_i 5.1 and 7.4 nM, respectively) and they also had anti-HIV activity in the cell-based assay, with EC₅₀ values down to 3.1 μM. However, relatively low potency was observed for compounds with cyclic P2 groups (K_i ca. 100 nM) [40]. Compounds **17a–b** with non-prime-side amino acid residues could interact with both S2 and S3 enzyme sub-sites, which is unfavorable for the cyclic P2 groups. These two features, suitable size of the

Synthesis of P1' elongated inhibitors



Biological data of selected inhibitors

Cmpd	4-R'	K_i (nM)	EC_{50} (μM)
14a ^a		2.1	1.0
14b		3.8	1.1
14c ^b		5.0	0.18
14d		12	0.90
15a ^c		12	> 10

^a CC_{50} 7.8 μM ; ^b P_{app} (Caco-2) = 33×10^{-6} cm/s and $C_{int} = 154 \mu L/min/mg$; ^c P_{app} (Caco-2) = 11×10^{-6} cm/s and $C_{int} = 190 \mu L/min/mg$

Fig. 11. Chemistry and biological evaluation of the *tert*-hydroxyethylhydrazide (type I) TS-mimicking HIV-1 PIs with P1' extensions.

iso-propyl group for the S2 pocket and appropriate S3 interactions, could be the reason for the potency of compounds **17a** and **17b**.

3.2.4. Central amide functionality

In an attempt to reduce the backbone for this class of TS mimics, we tested compounds **18a–b**, which had a central amide group instead of the hydrazide function [44]. Both compounds were biologically inactive, with K_i values >5 μM and EC_{50} values >10 μM ; hence, these compounds were not studied further (Fig. 13).

3.2.5. X-ray crystallography of the *tert*-hydroxyethylhydrazide (type I) TS-mimicking inhibitors

When compound **12a** (Fig. 10) was co-crystallized with HIV-1 protease, a 3D structure (PDB code 2cej, Fig. 14) [41] was obtained from the X-ray diffraction data [38,41]. The (S)-configuration at the quaternary carbon atom in the TS mimic was confirmed from the X-ray crystallography structure. It was observed that the tertiary hydroxyl group was hydrogen bound to one of the catalytically active aspartic acid residues (Asp125) residing in the enzyme's active site (Fig. 14), and hydrazide α - and β -nitrogens and Gly27 were involved in hydrogen bonding. Arg108 dictated the positioning of the P1' substituent, where the electronegative Br group was closely packed against the positively charged Arg side chain.

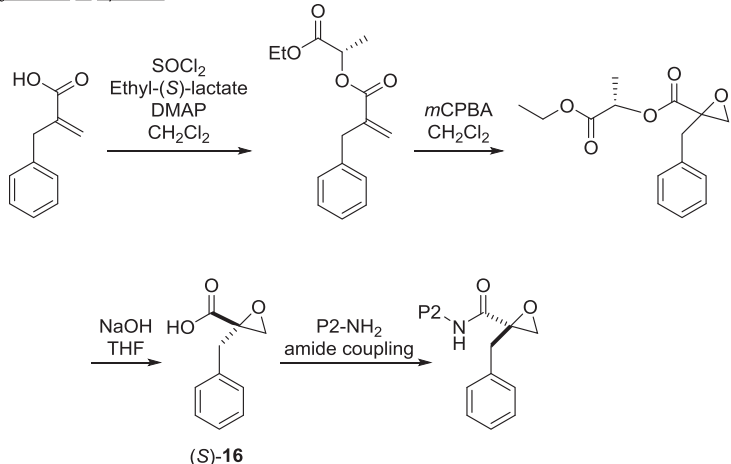
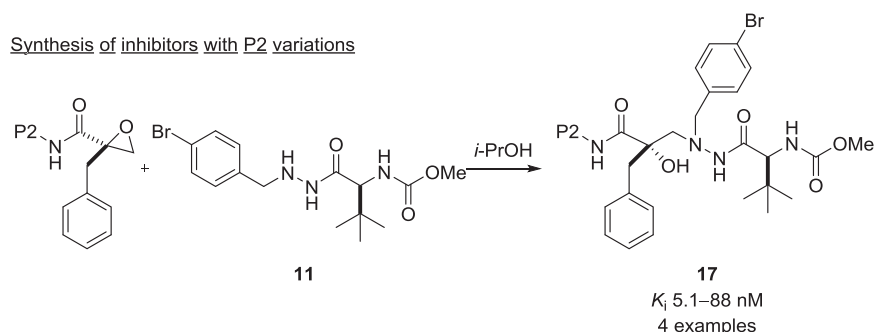
3.3. *Tert*-hydroxybutylhydrazide

As reviewed above, in Section 3.2, the first HIV-1 PI scaffold that used a tertiary alcohol as a TS mimic contained a one-carbon spacer between the tertiary alcohol and the hydrazide group. In order to improve the binding properties of the inhibitor to the catalytically active site of the aspartic acid, we extended the length of the inhibitor backbone to three carbon atoms, with the first study published in 2008 [43]. The SAR investigation, including organic syntheses, biological evaluations and X-ray crystallography studies with *tert*-hydroxybutylhydrazide TS mimics (three-carbon spacer), is presented in this section.

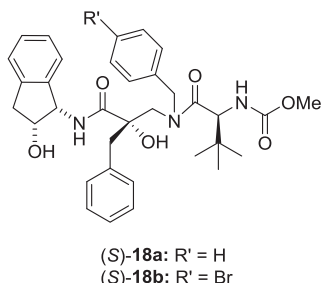
3.3.1. Variations in the P1' moiety

A library of synthesized compounds with different aromatic P1' substituents [43], prepared using palladium-catalyzed, microwave-assisted coupling reactions and the biological activities of these PIs, in terms of the inhibitory potency of the protease and the antiviral activity in the cell-based assay, are described here.

The non-prime side with the three-carbon spacer was synthesized according to Fig. 15 [43], starting from the commercially available (S)-2-hydroxy-3-phenylpropionic acid **19**. First, 2,2-dimethoxypropane **20** was used to protect the alcohol and acid functionalities in **19** and the obtained intermediate **21** was reacted with methyl acrylate **22**. Intramolecular lactone formation with a methyl ester from deprotection of the dioxolane **23**, followed by

Synthesis of epoxideSynthesis of inhibitors with P2 variationsBiological data of selected inhibitors

Cmpd	P2	K_i (nM)	EC_{50} (μM)
17a	MeO- $\text{CH}_2-\text{CH}_2-\text{NH}-$ (<i>R</i>)-	5.1	3.1
17b	(<i>R</i>)-	7.4	7.3

Fig. 12. Chemistry and biological evaluation of the *tert*-hydroxyethylhydrazide (type I) TS-mimicking HIV-1 PIs with variations in the P2 moiety.**Fig. 13.** HIV-1 PIs 18a–b.

peptide coupling with (1*S*,2*R*)-1-amino-2-indanol **6**, resulted in the cyclic compound **24** as a mixture of diastereomers. Intermediate (*R*)-**24** with the preferred stereochemistry at the quaternary carbon was protected by *tert*-butyldimethylsilyl (TBS)

trifluoromethanesulfonate and separated by column chromatography. Subsequently, reduction of the lactone and a protection-deprotection sequence led to the alcohol (*R*)-**25**. Initially, L-*tert*-leucine was selected as the P2' group and methyl carbamate as the P3' group for the prime side of the inhibitors, based on early studies on inhibitors in cell-based assays [38,41,89]. A series of hydrazides was synthesized to investigate the effects of various alkyl-, aryl- and biaryl components in P1'. β -Nitrogen-alkylated compounds **28** that contained P1' precursor groups, with variations in the size, polarity and hydrogen-bonding potential, were obtained via reductive amination of primary hydrazide **27** with various aldehydes **26** (Fig. 15) [43]. The desired inhibitors **29** were synthesized by Dess–Martin periodinane oxidation of (*R*)-**25**, followed by reductive amination of the corresponding aldehyde and hydrazides **28** [95].

Biological inhibitory data for selected compounds from this series with variations at the P1' site are shown in Fig. 15. All of the compounds with a *R*-configuration at the tertiary alcohol and free

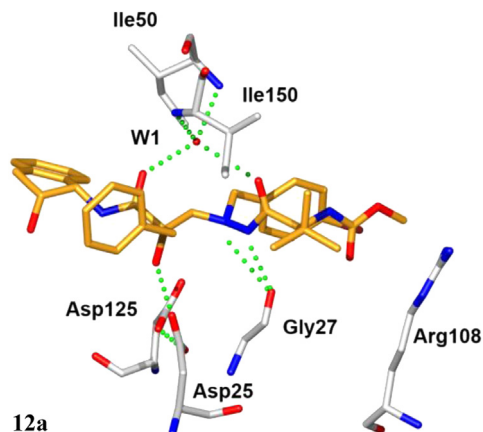
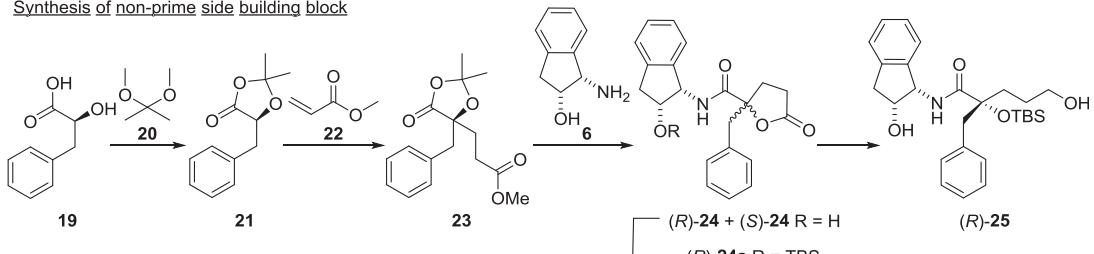


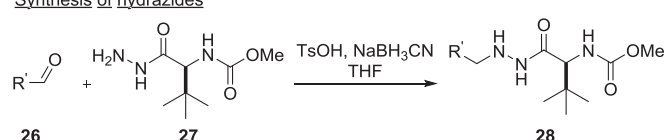
Fig. 14. X-ray crystallography structure of the 12a-HIV-1 protease complex; hydrogen bonds are highlighted as green dotted lines. Reproduced from Ref. [41] with permission from the American Chemical Society. (For interpretation of the references to color in this figure legend, the reader is referred to the web version of this article.)

hydroxyl groups, except one with a *tert*-butyl-substituted thiazole group at P1', exhibited relatively high potency against the HIV-1 protease, with K_i values of 2.3–11 nM [43]. It is worth noting here that the *R* stereochemistry of the *tert*-hydroxybutylhydrazide corresponds to the *S* stereochemistry of the tertiary alcohol for the *tert*-hydroxyethylhydrazide-based inhibitors. Poor inhibitory potencies were observed for compounds with small P1' groups, e.g. halogens or a cyano group in the 4-position of the P1' benzyl group (**29f–g**, EC₅₀ 1.2 and 0.85 μ M, respectively) and also for compounds with large and/or very lipophilic P1' groups. Intermediate potency (EC₅₀ 0.47–0.56 μ M) was observed for 4-substituted inhibitors with medium-sized groups such as 2-pyridyl (**29d**), as well as for the bicyclic **29b**. Compounds **29a**, **29c**, **29e** and **29h** were the most potent in the series (EC₅₀ 0.17–0.22 μ M); these contained relatively hydrophilic aromatic groups with heteroatoms in the second P1' aryl group. A compound containing 2-chloro-5-methoxy thiazole at the P1' position, which was inspired by a GlaxoSmithKline molecule structure [96], did not improve the cell activity (EC₅₀ 0.60 μ M). Surprisingly, in comparison to the 2-pyridyl inhibitor (**29d**), PIs

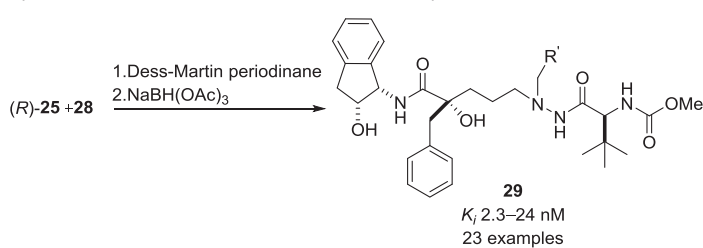
Synthesis of non-prime side building block



Synthesis of hydrazides



Synthesis of inhibitors with variations at the P1' moiety



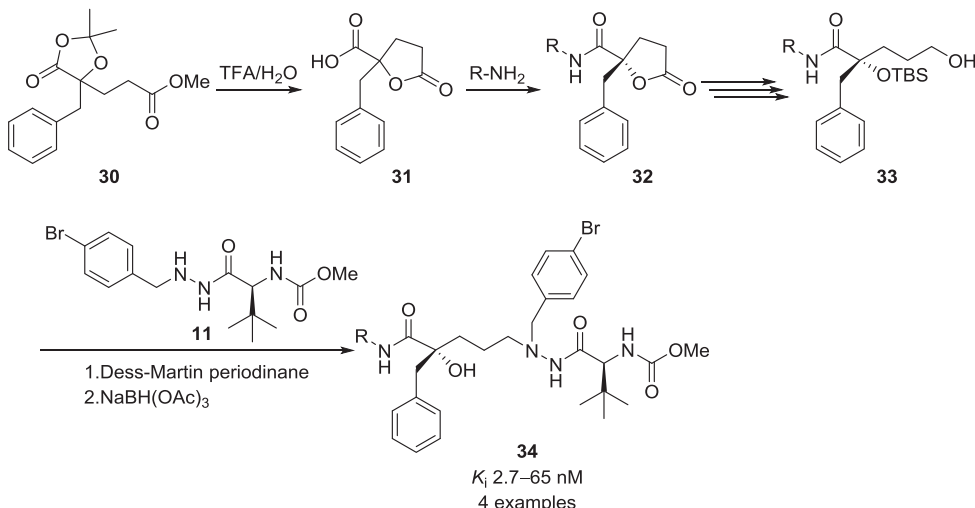
Biological data of selected inhibitors

Cmpd	R'	K_i (nM)	EC ₅₀ (μ M)	Cmpd	R'	K_i (nM)	EC ₅₀ (μ M)
29a ^a		2.3	0.21	29e		2.8	0.17
29b		2.3	0.48	29f		2.9	1.20
29c		2.4	0.22	29g ^a		3.3	0.85
29d		2.8	0.47	29h		3.3	0.17

^a P_{app} (Caco-2) = > 20 \times 10⁻⁶ cm/s.

Fig. 15. Chemistry and biological evaluation of the *tert*-hydroxybutylhydrazide TS-mimicking HIV-1 PIs with variations in the P1' moiety.

Synthesis of inhibitors with variations at the P2 moiety



Biological data of selected inhibitors

Cmpd	R	K_i (nM)	EC_{50} (μ M)
34a		2.7	2.1
34b		6.2	2.0 ^a

^a P_{app} (Caco-2) = 4.6×10^{-6} cm/s, C_{lnt} = 180 μ l/min/mg.

Fig. 16. Chemistry and biological evaluation of *tert*-hydroxybutylhydrazide TS-mimicking HIV-1 PIs with variations in the P2 moiety.

with 4-pyridyl (**29e**) (and 3-pyridyl) groups resulted in ca. 2.5-fold better cellular antiviral activity. In general, 50% of the cytotoxic concentration (CC_{50}) for all of the compounds in the series was $>10 \mu$ M. Inhibitors **29a** and **29g** had good permeation characteristics in the Caco-2 assay.

3.3.2. Variations in the P2 moiety

Since amino acid-derived P2–P3 substituents were successful in the approved inhibitor atazanavir [89,97], we became interested in developing a straightforward synthetic approach for the incorporation of new amino acid-derived P2–P3 groups. A library of compounds with various aromatic P1' substituents was therefore prepared in an attempt to optimize the most potent derivative in the P2–P3 series [45].

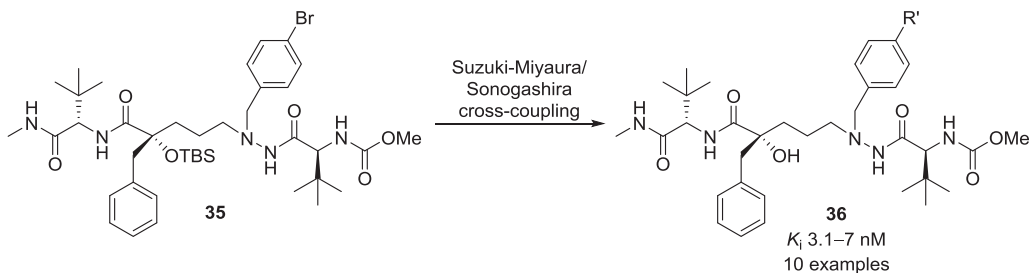
Inhibitors with variations at P2–P3 were synthesized in four steps, starting from compound **30** (Fig. 16) [45]. Intramolecular γ -lactone hydrolysis of **30** gave acid **31**. Compounds **32** were obtained by peptide coupling of the acid and various methyl-amide-derived amino acids. Further, the lactone moiety in **32** was reduced, the primary alcohol was protected by pivaloyl chloride, the tertiary alcohol was protected by TBS trifluoromethanesulfonate and the pivaloyl ester was reduced with lithium borohydride to provide compounds **33**. Oxidation of intermediates **33** by Dess–Martin periodinane followed by reductive amination with hydrazide **11** and finally TBS deprotection provided the desired compounds **34**.

Compound **34a** was very potent, with a K_i value of 2.7 nM, and no protease inhibition was observed for compound (*S*)-**34a**. *Tert*-

leucine-derived P2-group compound **34b** also had high potency (K_i 6.2 nM) and was the most active compound of the series in the cell-based antiviral assay, with an EC_{50} value of 2.0 μ M (Fig. 16). Inhibitors with long P2 side chains were the least active (K_i 65–170 nM) [45]. Interestingly, the indanol analog of **34b**, i.e. compound **29g**, had K_i and EC_{50} values of 3.3 nM and 0.85 μ M, respectively (Fig. 15). Attempts to preserve the hydrogen bonding property of the hydroxyl group that was seen in previously prepared inhibitors containing an amino-indanol-substituted P2–P3 fragment [38,41,43] were unsuccessful, as the corresponding compounds only poorly inhibited the enzyme and had no significant activity in the cell-based assay. Moreover, compound **34b** seemed to be similar to atazanavir in terms of Caco-2 permeation and stability (C_{lnt}) properties [38,98]. CC_{50} was $>10 \mu$ M for all the compounds in this series. X-ray crystallography studies were done after further optimization of **34b** with respect to P1' extension, as discussed in Section 3.3.5.

3.3.3. P1' extension

A SAR study was conducted, based on the idea that elongation of the P1' side chain could help the inhibitor to reach the S3' pocket, starting from compound **34b** with variations in the P1' moiety using palladium-catalyzed cross-couplings to extend the side chain. TBS-protected compound **35** was chosen as the arylpalladium precursor and Suzuki–Miyaura or Sonogashira cross-coupling reactions were performed to provide the desired compounds (Fig. 17) [45].

Synthesis of P1' elongated inhibitors

Biological data of selected inhibitors

Cmpd	R'	K_i (nM)	EC_{50} (μ M)
36a ^a		3.1	1.0
36b ^b		3.4	2.1
36c ^c		3.5	1.1
36d ^d		3.6	1.0
36e ^d		4.6	1.0

^a P_{app} (Caco-2) = < 1×10^{-6} cm/s, Cl_{int} = 63 μ L/min/mg;

^b P_{app} (Caco-2) = 6.1×10^{-6} cm/s, Cl_{int} = > 300

μ L/min/mg; ^c P_{app} (Caco-2) = 1.9×10^{-6} cm/s, Cl_{int} = 20

μ L/min/mg; ^d P_{app} (Caco-2) = 21×10^{-6} cm/s, Cl_{int} = >

300 μ L/min/mg.

Fig. 17. Chemistry and biological evaluation of *tert*-hydroxybutylhydrazide TS-mimicking HIV-1 PIs with P1' extensions.

Unexpectedly, no noteworthy considerable enhancement of the antiviral activity was observed for the compounds with elongated P1' side chains in comparison to compound **34b**, as shown in Fig. 17. The highest potency in the series was obtained by compound **36a**, with a K_i value of 3.1 nM and an EC_{50} value of 1.0 μ M. The K_i values for compounds **36a**, **36c** and **36d** were in the range of 3.1–3.6 nM, whereas further extension was tolerated but not helpful, as seen for compound **36b** (K_i 3.4 nM). The potency of the 3-pyridyl **36a** and 3-ethynyl pyridyl **36b** P1'-elongated inhibitors was similar to that of the corresponding 2-pyridyl and 4-pyridyl compounds. Further, P1' elongation, as seen in compound **36e**, increased Caco-2 cell permeation and decreased the metabolic stability (cf. Cl_{int}), whereas placing pyridyl at the P1' position (**36a** and **36c**) decreased the permeation but increased the metabolic stability. The cytotoxicity was >10 μ M for all the compounds in the series.

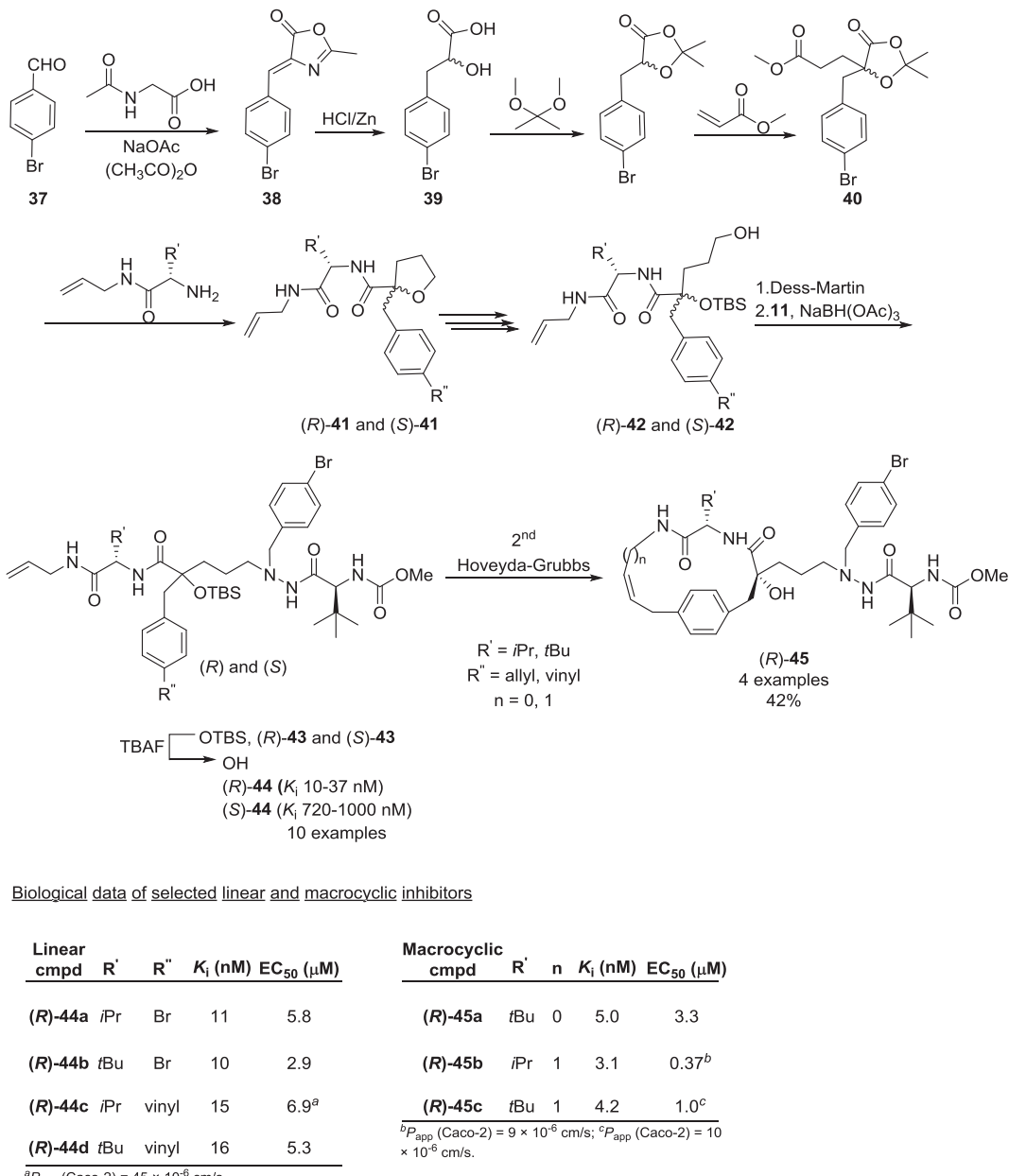
3.3.4. Variations in P1–P3 macrocyclization

Encouraged by the often positive pharmacokinetic and pharmacodynamic outcomes associated with various macrocyclizations of linear bioactive compounds [99], we decided to apply this strategy to prepare a new series [51] of HIV-1 PIs related to azanavir but containing a tertiary alcohol as part of the TS-mimicking core structure (Fig. 18) [41,100]. The presence of peptide bonds, high flexibility and exposure of polar functionalities in linear molecules can result in metabolic instability and poor membrane permeation, and macrocyclization of the linear peptides could help to reduce the peptidic characteristics associated with increased structural rigidity [101]. Cyclizations also provide better resistance to proteolytic digestion by facilitating internal hydrogen

bonding, thus helping to improve bioavailability and enabling the compound to reach its intracellular targets [99].

Although the macrocyclization strategy has been previously investigated for the design of HIV-1 PIs [102,103], no examples of macrocyclic tertiary alcohols had been reported at this stage. In our first attempt, we prepared a library of P1–P3 macrocycles including 14- and 15-membered rings with bromine at the *para* position on the P1' side [51]. The synthetic route is depicted in Fig. 18. Commercially available *p*-bromobenzaldehyde **37** was condensed with *N*-acetyl glycine and the resulting oxazolone **38** was reduced by treatment with hydrochloric acid/amalgamated zinc. The obtained diol **39** was protected using 2,2-dimethoxypropane followed by a lithium diisopropylamide-mediated conjugate addition with methyl acrylate providing the aryl bromide **40**, which was treated with trifluoroacetic acid resulting in the carboxylic acid. Coupling with amines furnished intermediates **41**. The lactone moiety of compounds (*R*)-**41** and (*S*)-**41** was reduced using lithium borohydride, followed by a couple of protection/deprotection steps on the primary and tertiary alcohols to give the precursor **42** for the substitution of the bromide on the P1 side. A vinyl group was introduced via a microwave-assisted Suzuki cross-coupling reaction [42,94,104] with the aim of preparing 14-membered macrocycles. The allyl group was introduced by a microwave-promoted Stille coupling [105], to obtain 15-membered macrocycles.

Oxidation of intermediate alcohol **42** by Dess–Martin periodinane followed by reductive amination with hydrazide **11** and final TBS deprotection provided the desired linear compounds **44**, which were used as precursors for the macrocyclization via microwave-

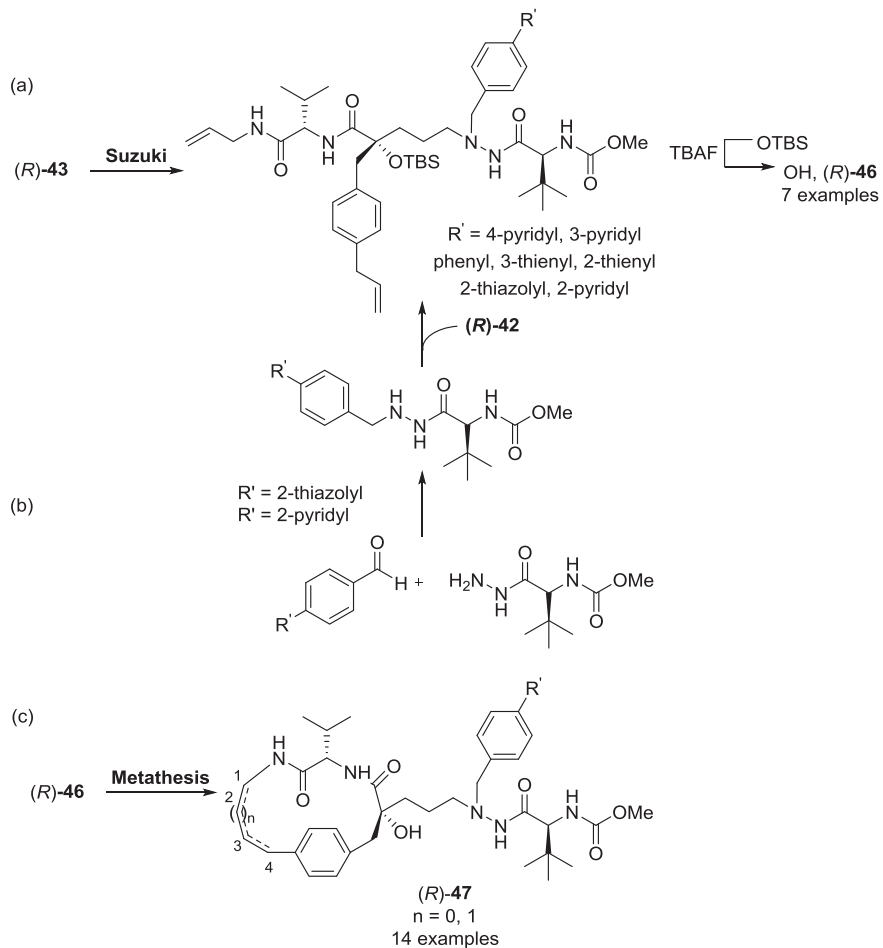
Synthesis of P1-P3 macrocyclic inhibitors**Fig. 18.** Chemistry and biological evaluation of the *tert*-hydroxybutylhydrazide TS-mimicizing HIV-1 PIs with macrocyclization of P1–P3.

induced ring-closing metathesis using the second generation Hoveyda-Grubbs catalyst [106].

The HIV-1 protease inhibition and antiviral activity of both linear (R)-44 and (S)-44 and macrocyclic (R)-45 compounds were evaluated; the most significant results are shown in Fig. 18. All linear compounds with an R configuration of the tertiary alcohol had strong inhibition profiles ($10 \text{ nM} \leq K_i \leq 37 \text{ nM}$) whereas compounds with an S configuration were inactive, with K_i values up to 100 times higher ($720 \text{ nM} \leq K_i \leq 1000 \text{ nM}$). These results were expected from our previous studies [40,43]. The macrocycles furnished 2- to 3-fold better K_i values than the linear compounds as well as improved EC_{50} values (down to $0.37 \mu\text{M}$). It is worth noticing that the linear PIs permeated well ($P_{app} > 40 \times 10^{-6} \text{ cm/s}$) in the Caco-2 assay and macrocycles (R)-45b and (R)-45c had low

EC_{50} values (0.37 – $1.0 \mu\text{M}$) with satisfactory permeation ($P_{app} = 9$ – $10 \times 10^{-6} \text{ cm/s}$).

Although the best macrocycles in this study had lower EC_{50} values than the corresponding linear compounds, the potency enhancement was only modest. Therefore, we decided to optimize the P1' position by introducing (hetero)aromatic moieties [107]. The P1' substituents were introduced via Suzuki-Miyaura cross-coupling using their respective boronic acids, Herrmann's palladacycle (as a palladium precatalyst) and the pre-ligand tri(*tert*-butyl)phosphonium tetrafluoroborate [108–110], or palladium(II) acetate as catalyst and triphenylphosphine as ligand (Fig. 19, a) [111]. However, these protocols were both unsuccessful when the cross-coupling reaction was performed with 2-(pyridyl/thiazolyl) boronic acids, possibly due to rapid protodeboronation and/or

Synthesis of P1' elongated inhibitors and P1–P3 macrocyclization

Biological data of selected inhibitors

Linear Cmpd	R'	K _i (nM)	EC ₅₀ (μ M)	Macrocyclic Cmpd	n	K _i (nM)	EC ₅₀ (μ M)
(R)-46a	4-pyridyl	7.8	0.81 ^a	(R)-47a	1	5.4	0.13 ^c
(R)-46b	2-thiazolyl	8.0	2.7 ^b	(R)-47b	1	2.2	0.2 ^d
^a P _{app} (Caco-2) = 22 × 10 ⁻⁶ cm/s; ^b P _{app} (Caco-2) = 47 × 10 ⁻⁶ cm/s.							
^c P _{app} (Caco-2) = < 1 × 10 ⁻⁶ cm/s; ^d P _{app} (Caco-2) = 2.2 × 10 ⁻⁶ cm/s; ^e P _{app} (Caco-2) = 2 × 10 ⁻⁶ cm/s.							
(R)-47c	2-pyridyl	3.6	0.19 ^e				

Fig. 19. Chemistry and biological evaluation of the P1'-functionalized *tert*-hydroxybutylhydrazide TS-mimicking HIV-1 PIs with macrocyclization of P1–P3.

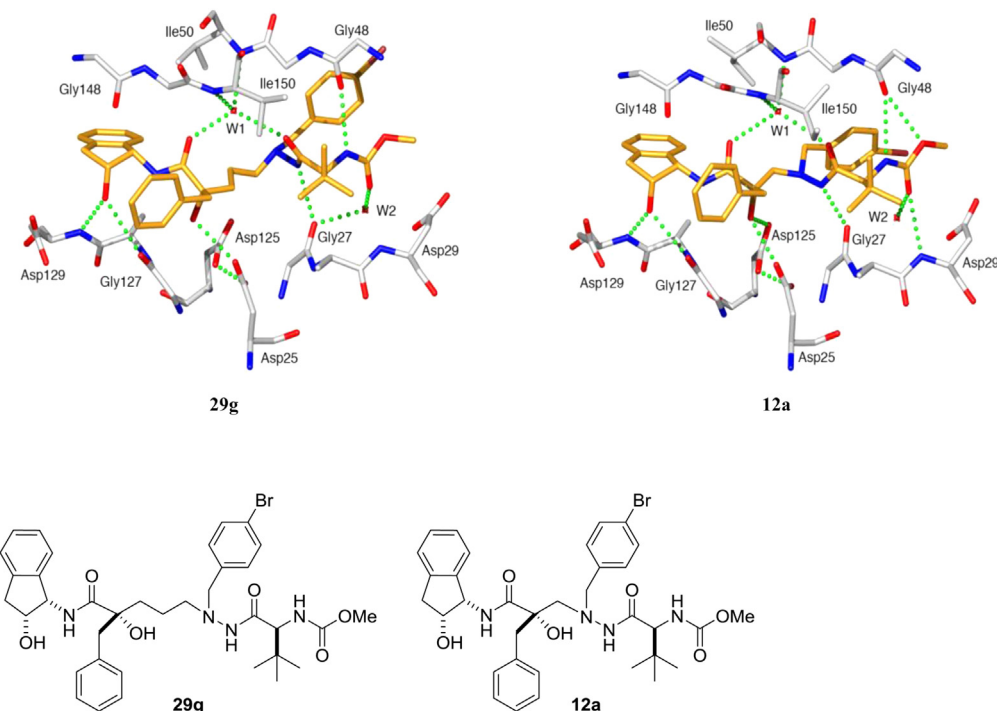


Fig. 20. X-ray crystallography structures of compounds **29g** and **12a** co-crystallized with HIV-1 protease, showing the active site of the protease. Reproduced from Ref. [43] with permission from the American Chemical Society.

polymerization [112–114]. Thus, a different approach, using pre-synthesized diaryl aldehydes, was chosen to introduce the 2-pyridyl and 2-thiazolyl moieties into the P1' position (Fig. 19, b) [107]. Deprotection of the TBS-protected tertiary hydroxyl group, using tetrabutylammonium fluoride at room temperature, furnished the desired linear inhibitors (*R*)-**46** with high yields.

Macrocyclization of linear inhibitors (*R*)-**46** was thereafter performed via a microwave-induced ring-closing metathesis reaction (Fig. 19, c) [115,116]. Fourteen-membered macrocycles were obtained as, in some cases, the reactions gave a mixture of isomers because of double-bond migration and ring-contraction reactions [117–119].

In almost all cases, the P1–P3 macrocyclization approach furnished improved inhibitors **47** in terms of inhibition potency and antiviral activity (Fig. 19), with K_i values in the range of 2.2–31.5 nM and EC₅₀ values in the range of 0.13–3.05 μ M. The macrocycle with a phenyl moiety at the P1' position was the only exception and this was the least potent inhibitor in this series (K_i 120 nM and EC₅₀ 7.35 μ M) [107]. As expected from our previous study [51], the 14-membered macrocycles were, in all cases, less potent than the corresponding 15-membered cyclic inhibitors. Double-bond migration from the 2,3 to the 1,2 position of the 15-membered macrocycles did not strongly affect the inhibition profile, as the inhibitors had similar K_i values. Macroyclic molecules containing 2-thiazolyl or 2-pyridyl groups were highly potent; **47b** was the best inhibitor (K_i 2.2 nM) and also had very good antiretroviral activity (EC₅₀ 0.2 μ M).

3.3.5. X-ray crystallography of the tert-hydroxybutylhydrazide TS-mimicking inhibitors

X-ray crystallography results showing the arrangement of the benzyl bromide compound **29g** (PDB ID 2uxz) (Fig. 15) and compound **12a** (one-carbon spacer, Fig. 10, PDB-ID 2bqv) and the relevant hydrogen bonds to the enzyme amino acid residues from the active site of the PI are shown in Fig. 20 [43]. Compound **29g**

had 54 contact points with the protein and compound **12a** had 48 contact points. There were five direct hydrogen bonds between compound **29g** and the protein, and three bonds via water molecules. The tertiary alcohol of **29g** could form a hydrogen bond to only one of the aspartic residues in the active site, possibly because of their extended central carbon skeleton; in comparison, **12a**, could form hydrogen bonds to both of the aspartic residues (although the bond to Asp125 was weak, with a binding distance of 3.3 Å). Compound **29g** had a relatively strong interaction with Asp25 (2.9 Å) and the *para*-bromo atom on the P1' benzyl group was directed towards the solvent. The bromine atom in inhibitor **12a** had four close-packed contact points with the lining residues.

X-ray crystallography data were obtained for nine (four linear and five macrocycle) P1'-functionalized inhibitor/HIV-1 protease complexes [107]. A detailed comparison of linear and macrocyclic scaffolds was carried out and the global effect of the macrocyclization approach on the binding profiles of the inhibitors was analyzed (Fig. 21). The linear and macrocyclic scaffolds bound in a similar fashion to the enzyme with only minor differences. The main effect of the macrocyclization seems to be that the introduced constraints made the macrocycles slightly more compact than the corresponding linear analogs, which translates to a better fitting of the macrocycles. Interestingly, this improved accommodation of the macrocyclic structures at the non-prime site of the enzyme affected the hydrogen-bonding distances between the tertiary hydroxyl group in the PIs and the aspartic residues Asp25/Asp125 and Gly27 in the active site of the enzyme.

The adjustment of the macrocyclic scaffold in the P1–P3 region was also reflected in the rotation of the iso-propyl group at the P2 pocket. For the P1–P3 macrocyclic compounds, the iso-propyl group appeared to be forced to point away from the nitrogen as the iso-propyl group was closer to the backbone of the protein. The groups in the P1 and P3 positions of the linear compounds did not seem to interact closely with the protein. In contrast, the two allyl

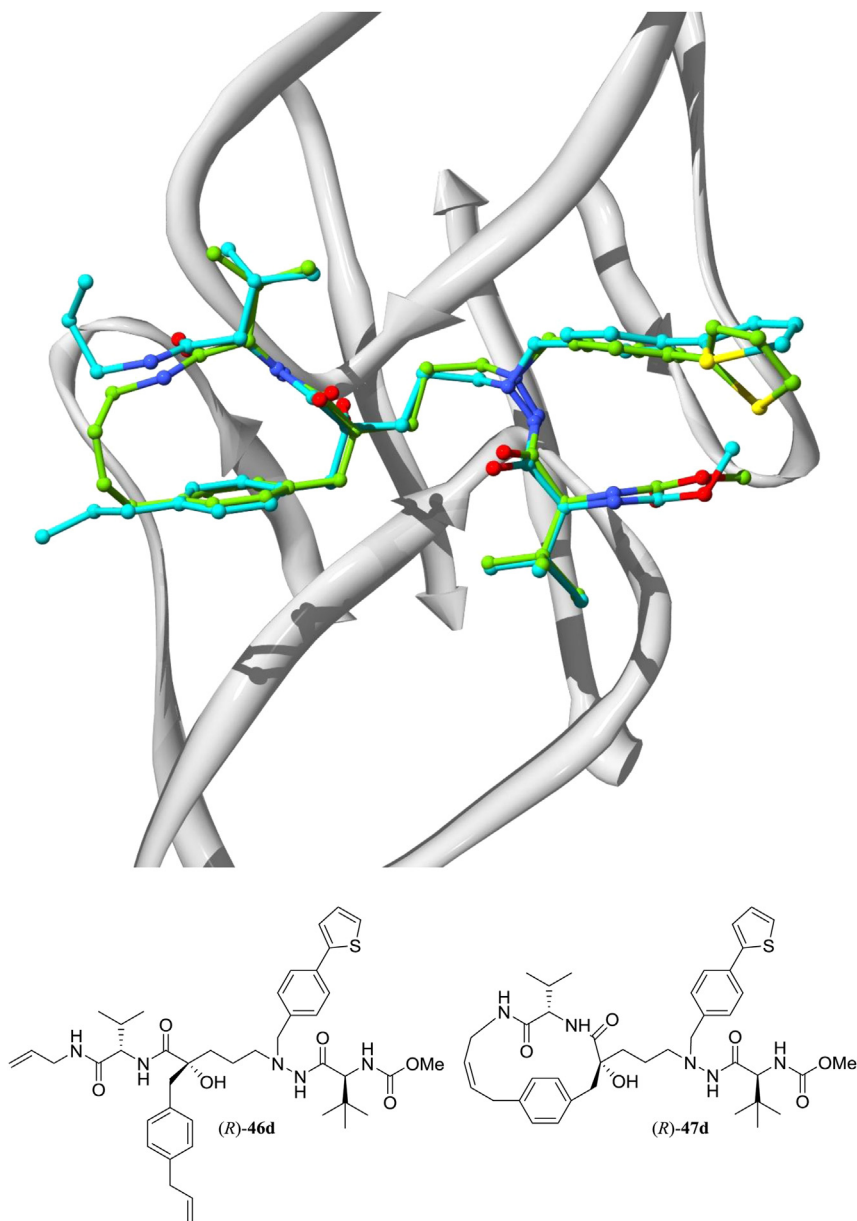


Fig. 21. Comparison of the non-cyclic (*R*)-46d (PDB ID 4cpr, turquoise) and the corresponding macrocycle (*R*)-47d (PDB code: 4cpx, green) complexes. The macrocyclic compound mimicked the binding of the linear PI very well, differing significantly only at the point of macrocyclization at the S3 site and at the hetero-aromatic substituent at the S1' site, the latter having partial rotational freedom. Reproduced from Ref. [107] with permission from the American Chemical Society. (For interpretation of the references to color in this figure legend, the reader is referred to the web version of this article.)

groups in both the P1 and P3 positions seemed to be more flexible and were directed away from the protein surface [107].

3.4. *Tert-hydroxypropylhydrazide*

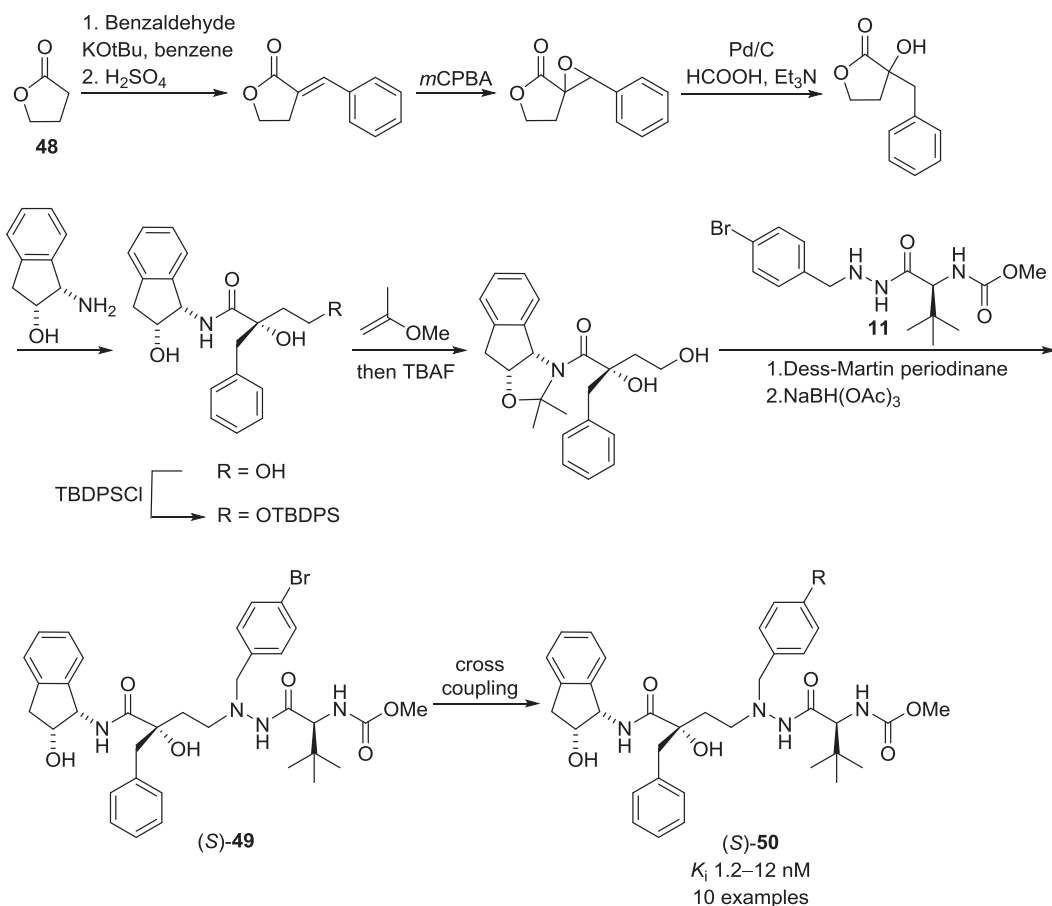
As reviewed in Sections 3.2 and 3.3, the HIV-1 PIs with one or three carbon spacers were potent inhibitors, with K_i values down to 2.1 nM and good Caco-2 membrane permeation. However, the linear compounds containing these TS mimics had only moderate cellular antiviral activities, with the best EC₅₀ value of 170 nM (compounds 29e and 29h, Fig. 15) and poor stability in liver microsomes. It therefore seemed logical to prepare new molecules with a TS mimic containing a two-carbon spacer between the quaternary carbon and the hydrazide β -nitrogen. This was mainly because X-ray crystallography data from the previous two

categories of inhibitors (one and two carbon spacers, Sections 3.2 and 3.3), in combination with modeling studies, indicated that a two-carbon distance would bring the OH group nearer to Asp25 at the active site, which might increase the potency as a result of the stronger interaction.

3.4.1. Variations in the P1' moiety

The first aim of our SAR study of the *tert*-hydroxypropylhydrazide class of inhibitors was to optimize the nature of the group at the P1' site in an attempt to improve the cell-based antiviral activity.

Commercially available γ -butyrolactone **48** was used to synthesize bromides (*S*)-**49** and (*R*)-**49** (Fig. 22), which were separated by column chromatography and used as aryl precursors for cross-coupling reactions to obtain a series of *para* P1'-extended

Synthesis of inhibitors with variations at the P1' moietyBiological data of selected inhibitors

Cmpd	R	K_i (nM)	EC_{50} (nM)	CC_{50} (μ M)
(S)-50a		2.9	40	7.9 ^a
(S)-50b		1.7	7	> 10 ^b
(S)-50c		1.2	9	4.9 ^c

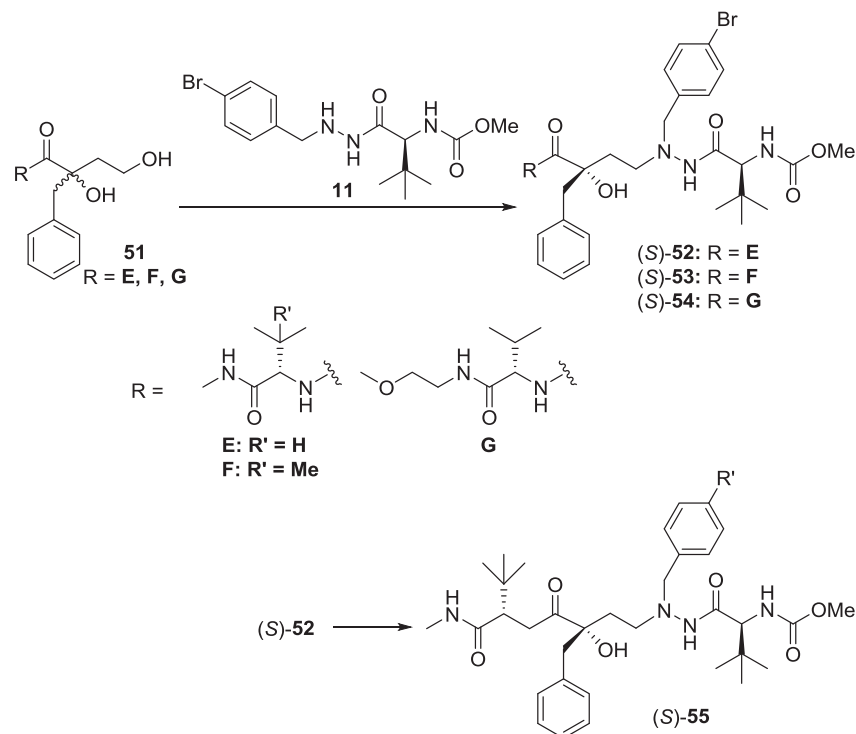
^a P_{app} (Caco-2) = 42×10^{-6} cm/s, $Cl_{int} > 300 \mu$ L/min/mg;
^b P_{app} (Caco-2) = 3.5×10^{-6} cm/s, $Cl_{int} = 20 \mu$ L/min/mg; ^c P_{app} (Caco-2) = 26×10^{-6} cm/s, $Cl_{int} > 300 \mu$ L/min/mg.

Fig. 22. Chemistry and biological evaluation of the *tert*-hydroxypropylhydrazide TS-mimicking HIV-1 PIs with variations in the P1' moiety.

inhibitors **50**, having retained the *S* or *R* configuration at the quaternary carbon. Pyridine compounds **50b** and **50c** were synthesized by Stille couplings [109], using the corresponding tributyltin reagents [44].

The antiviral activities of the *S* compounds **50a**, **50b** and **50c** are summarized in Fig. 22 [44]. All of the compounds in the series had high potencies, with K_i values in the range of 1.2–12 nM. When (*R*)-**50a** was tested for antiviral activity it was seen to be inactive, with a K_i value > 5 μ M. P1' substitution of the *S* isomer distinctly influenced the cell activity and high antiviral activity (EC_{50} 3–13 nM)

was observed for all the tested 4-aryl-elongated compounds, except for the *N*-(4-phenyl)acetamide (compound **16** in an earlier paper [44]). Cytotoxicity ($CC_{50} < 10 \mu$ M) was exhibited by the bromo- ((*S*)-**50a**) and 3-pyridyl- ((*S*)-**50c**) substituted compounds (CC_{50} 7.9 and 4.9 μ M, respectively). A stability test using a liver microsome homogenate was performed on the 2-pyridyl derivative (*S*)-**50b** (the best compound in this series, according to the $K_i/EC_{50}/CC_{50}$ profile), its parent compound (*S*)-**50a** and the related inhibitor (*S*)-**50c**. Compound (*S*)-**50b**, with the atazanavir prime side, was relatively more resistant to degradation by metabolic enzymes

Synthesis of inhibitors with variations at the P2 moiety

Biological data of inhibitors (S)-52–55

Cmpd	R	R'	K _i (nM)	EC ₅₀ (nM)	Cmpd	R'	K _i (nM)	EC ₅₀ (nM)
(S)-52	E	Br	1.7	72	(S)-55a		1.1	47
(S)-53	F	Br	2.9	160	(S)-55b		1.0	37
(S)-54	G	Br	3.2	170	(S)-55c		2.0	40

Fig. 23. Chemistry and biological evaluation of the *tert*-hydroxypropylhydrazide TS-mimicking HIV-1 PIs with variations in the P2 moiety.

(C_{int} 20 $\mu\text{L}/\text{min}/\text{mg}$), while compounds (S)-50a and (S)-50c degraded rapidly ($C_{\text{int}} > 300 \mu\text{L}/\text{min}/\text{mg}$). However, excellent Caco-2 membrane permeation was observed for compounds (S)-50a and (S)-50c, with P_{app} values of $42 \times 10^{-6} \text{ cm/s}$ and $26 \times 10^{-6} \text{ cm/s}$, respectively; compound (S)-50b had a slower penetration with a P_{app} of $3.5 \times 10^{-6} \text{ cm/s}$.

Encouraged by the enzyme inhibition data, antiviral activity and cell toxicity properties, compounds (S)-50a, (S)-50b and (S)-50c were subsequently tested against selected PI-resistant isolates of HIV-1 (Table 1) [44]. Incubation of the cell-free virus with increasing concentrations of inhibitors saquinavir (entries 2 and 3 in Table 1) and ritonavir (entries 5 and 6) induced clinically relevant mutations in the HIV-1 protease genome to acquire the desired resistant isolates. In comparison to the wild-type enzyme, the three S inhibitors had equal or greater potency against the viral isolate with G48V and L90M mutations in the protease, which generally occur in saquinavir-treated patients [120]. Inhibitors (S)-50a, (S)-50b and (S)-50c were highly potent against one of the isolates containing V82A and M46I mutations and (S)-50b was equipotent against this isolate and the wild-type isolate (entry 4). The

mutations V82A and M46I, located at the protease S1' site and in the flap region, respectively, are known to cause resistance against several of the FDA-approved HIV-1 PIs [85,86]. The four universal protease-associated mutations (UPAMs) occur at amino acids 33, 82, 84 and 90; these are usually observed in patients with disease

Table 1
Antiviral activity against selected HIV-1 PI-resistant isolates and inhibition data.

Entry	Mutations in protease	EC ₅₀ (μM)		
		(S)-50a	(S)-50b	(S)-50c
1	Wild-type (wt)	0.040	0.007	0.009
2	G48V, L90M	0.008	0.008	0.010
3	A71V, I84V L90M	0.044	0.007	0.019
4	V32I, M46I A71V, V82A	0.070	0.006	0.014
5	V32I, M46I V82A	0.074	0.024	0.027
6	M46I, V82F, I84V	0.24	0.13	0.60
7 ^a	L63P, V82T, I84V	30	16	16

^a Atazanavir $K_i = 6.5 \text{ nM}$.

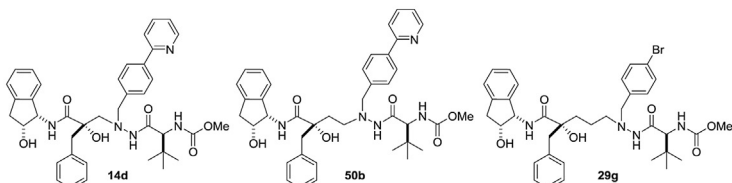
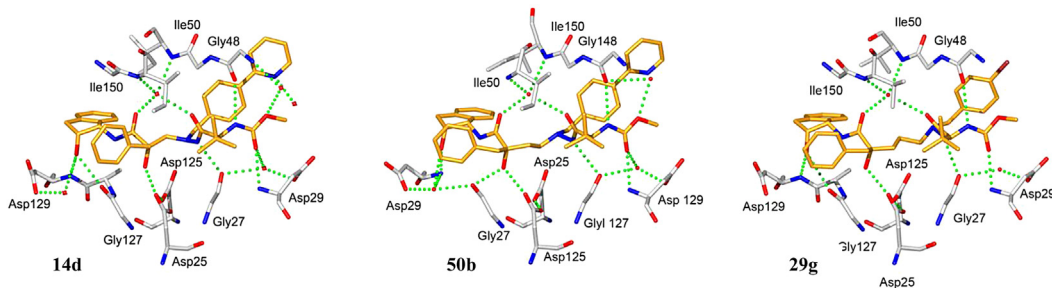


Fig. 24. X-ray crystallography structures of **14d**, **50b** and **29g** co-crystallized with HIV-1 protease. Reproduced from Ref. [44] with permission from the American Chemical Society.

resistant to HIV therapy [120]. The three PIs were relatively potent in the presence of one (entries 2, 4 and 5) or two (entry 3) UPAMs; however, there was a loss of potency in the presence of the mutation involving residues 82 and 84 (entry 6).

3.4.2. Variations in the P2 moiety

The indanolamine moiety in some of the synthesized inhibitors was metabolically unstable because of the propensity of the indan to undergo 3'-hydroxylation [90,91]. Inhibitors with variations in the P2 moiety were therefore synthesized and investigated (compounds **52–54**, Fig. 23) [44].

Compounds **52–54** were prepared via a coupling reaction from the starting materials **51** and the hydrazine **11**. Compound (*S*)-**52** was then used as a precursor for the Suzuki and Stille cross couplings to obtain the desired compounds **55a–c** (Fig. 23) [44].

Compounds with P2 variations (**52–55**, with an *S* configuration at the tertiary alcohol) were highly potent against the protease. K_i values ranged from 1.0 nM (compound **55b**) to 3.2 nM (compound **54**) and the compounds had good antiviral activity (EC₅₀ 37–170 nM, Fig. 23) [44]. However, none of these compounds (**52–55**) showed any improvement in their $K_i/\text{EC}_{50}/\text{CC}_{50}$ profiles over compound (*S*)-**50b** (Fig. 22). Hence, this series of compounds was not evaluated further, in terms of either biological activity or X-ray crystallography.

3.4.3. X-ray crystallography of the tert-hydroxypropylhydrazide TS-mimicking inhibitors

X-ray crystallography structures of compounds **50b** (two-carbon spacer, Fig. 22, PDB code 2wkz), **14d** (one-carbon spacer, Fig. 11, PDB code 2cem) and **29g** (Fig. 15, three-carbon spacer, PDB code 2uxz)

are depicted in Fig. 24 [44]. In comparison to the **14d**- and **29g**-enzyme complexes, compound **50b** was rotated 180° at the active site. Compounds **50b** and **14d** had a shorter binding distance (2.7 Å) from the tertiary alcohol to Asp 25/125 than compound **29g** (2.9 Å to Asp25). Compound **50b** formed one hydrogen bond from the indanolamine hydroxy group to the backbone NH group of Asp29 (3.0 Å) and another hydrogen bond to a water molecule (3.1 and 2.8 Å), whereas there were two hydrogen bonds from the indanolamine hydroxyl group to Gly127 and Asp129 in compounds **14d** and **29g**. The tertiary alcohol in **50b** was hydrogen bonded to the backbone carbonyl of Gly27 (2.6 Å), but this was more difficult in **14d** as the hydroxyl group was too far away (3.3 Å). There were seven and five hydrogen bonds to the protein and via water molecules, respectively, for **50b**, six and five for **14d**, and five and three for **29g**. The arrangement of the hydrogen bonds between the conserved water molecule and the non-prime-side amide carbonyl, the hydrazide carbonyl, and the enzyme backbone NH groups of Ile50 and Ile150 was similar for compounds **50b**, **14d** and **29g**.

3.5. Current status and prospects

We have reviewed a relatively new generation of HIV-1 PIs containing tertiary-alcohol-based TS mimics. The inhibitors have been classified according to the number of carbons used to elongate the core structure: one (*tert*-hydroxyethylhydrazide), two (*tert*-hydroxypropylhydrazide) or three (*tert*-hydroxybutylhydrazide). The PIs in the two-carbon spacer series were more potent inhibitors of HIV-1 protease; the best compound, **50b**, which had a pyridine in the P1' terminal substituent, had a K_i value of 1.7 nM. However, inhibitor **50b** was slightly less potent than atazanavir (K_i 0.5 nM) and indinavir (K_i 0.3 nM) (Fig. 5). The higher inhibition potency of

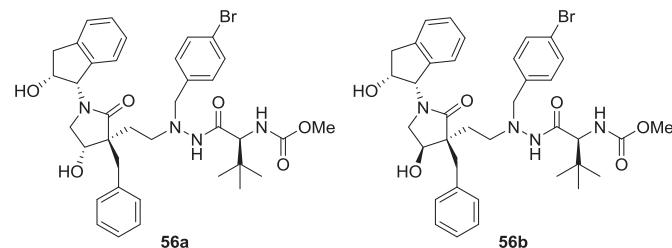


Fig. 25. Lactam-based HIV-1 PIs **56a** and **56b**.

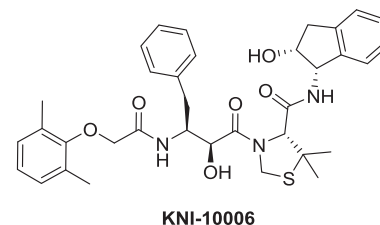
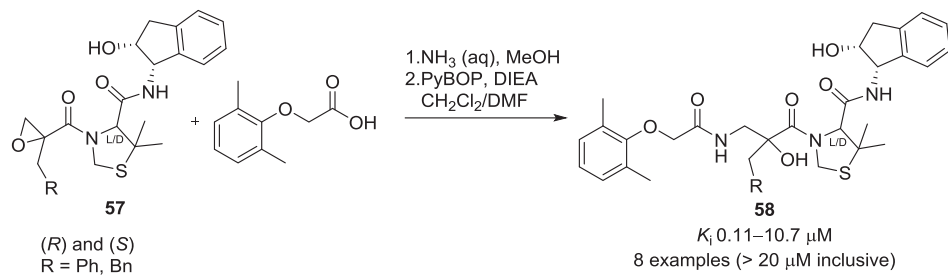
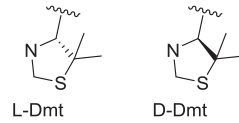


Fig. 26. Norstatine-based plasmeprin inhibitor KNI-10006.

Synthesis of inhibitors containing a *tert*-hydroxy- α -alkylnorstatine TS mimick

Biological data of selected inhibitors

Cmpd	R, L/D	K_i (μM)				
		PfPM2	PfPM4	PmPM4	PoPM4	PvPM4
(S)-58	Ph, L-Dmt	> 20	0.70	0.26	0.11	0.16
(R)-58	Ph, L-Dmt	> 20	0.72	0.25	0.53	0.19


Fig. 27. Chemistry and biological evaluation of the *tert*-hydroxy- α -alkylnorstatine TS-mimicking plasmeprin inhibitors.

the two-carbon spacer series was also supported by the X-ray crystallography results; Fig. 24 shows inhibitor **50b** co-crystallized with HIV-1 protease. The tertiary alcohol had hydrogen bonds not only to Asp125, but also to the Gly27 carbonyl in the protein backbone. The P1 substituent of **50b** also fit the S1 and S3 pockets of the enzyme better, as seen from the improved interaction with Val182 and Arg108.

The EC₅₀ values were in general more than 20-fold better for the inhibitors with two-carbon spacers than for those with one- or three-carbon spacers, probably due to improved masking by the tertiary alcohol of the former. For example, with pyridine as the P1' substituent, the EC₅₀ value for inhibitor **50b** (Fig. 22) was 7 nM, while the values for the one- and three-carbon spacer inhibitors were 180 nM (compound **14c**, Fig. 11) and 170 nM (**29e**, Fig. 15), respectively. Notably, as shown by the antiviral cell-based assay, inhibitor **50b** had better antiviral activity than indinavir (EC₅₀ 50 nM) and similar activity to atazanavir (EC₅₀ 8 nM), lopinavir (EC₅₀ 10 nM) and darunavir (EC₅₀ 4 nM). A significant improvement in the EC₅₀ values was obtained by the macrocyclization approach at the P1–P3 site; the EC₅₀ value for the three-carbon-tethered compound **47b** (Fig. 19) was 0.2 μM and the K_i value was 2.2 nM, whereas the corresponding values for the non-cyclized inhibitor **46b** were EC₅₀ 2.7 μM and K_i 8.0 nM.

Inhibitor **50b** had a low C_{int} (20 $\mu\text{L}/\text{min}/\text{mg}$) in the liver microsome assay, which is considered to be promising. It has been previously established that HIV-1 PIs are rapidly metabolized/degraded by cytochrome P450 enzymes, which means that they have low oral bioavailability [121]. Nevertheless, the known metabolic problems associated with the indanolamine moiety required further investigation. The inhibitors obtained when the indanolamine was replaced by *N*-alkylated amino acid-based moieties were less potent. Further, the enzyme assay results with HIV-1 protease-resistant viral isolates were favorable for inhibitor **50b**, except when there were mutations at residues 82 and 84 (Table 1), probably because of the loss of hydrophobic interactions, as seen from the co-crystallized X-ray structures (Fig. 24).

Based on this evidence, it can be concluded that PI **50b** is a highly promising lead structure in the field of development of new HIV-1 PIs. It was considered worthwhile establishing stronger

symmetric hydrogen bonds in the new inhibitors, to both the catalytic residues of the protease, Asp 25 and Asp 125. With this in mind, we have recently developed a strategy for relocating the hydroxyl group one position away from the backbone, thus further strengthening the central TS mimic. In the first series of examples, we prepared inhibitors with a β -hydroxy γ -lactam group containing a *sec*-hydroxy and a two- or three-carbon spacer [46]. Functionalization of the two most potent inhibitors (*3R,4S*)-**56a** and (*3R,4R*)-**56b** (Fig. 25) by heteroaromatic moieties in the *p*-benzyl P1' position provided compounds with K_i values down to 0.7 nM and EC₅₀ values down to 40 nM. However, this strategy will not be further discussed in this review as it does not involve a tertiary alcohol as the TS mimic. Nonetheless, it is felt that combining tertiary alcohol TS-mimicking structures with stereopure lactam-based moieties that also provide rigidity to the backbone of the inhibitor could be a potential path to follow. An alternative strategy for improving the pharmacokinetic profile and potency of the inhibitors could be macrocyclization at the P1–P3 site of the two-carbon spacer series, in particular for compound **50b**.

4. Plasmeprin inhibitors

4.1. Background

Malaria, one of the earliest diseases known to man, is endemic in more than 100 countries. Despite considerable scientific advances and the development of modern drugs, more than three billion people are still living under the threat of malarial infection. The WHO estimated that ca. 200 million clinical cases occurred globally in 2012, resulting in nearly half a million deaths [122]. Malaria in humans is caused by four species of protozoal parasites of the *Plasmodium* genus, *Plasmodium falciparum* (Pf), *Plasmodium malariae* (Pm), *Plasmodium ovale* (Po) and *Plasmodium vivax* (Pv); of these, Pf is responsible for most malarial fatalities. *Plasmodium* parasites are spread by female mosquitoes of the genus *Anopheles*. Parasitic strains resistant to the currently available antimalarial drugs are evolving at an alarming rate, indicating an acute need for new therapeutic agents [122,123].

Sequencing of the Pf genome revealed a number of promising new drug targets for treating malaria [124–126]. For example, the enzymes used by the parasites to degrade hemoglobin into smaller peptides and amino acids have been investigated as potential antimalarial targets. Four of these, the APs plasmepsin I, II and IV and the histo-aspartic protease HAP, are known to be involved in hemoglobin degradation in the parasite digestive vacuole (DV) [127–129]. Orthologs of only the Pf plasmepsin IV (PfPM4) have been identified in the other three human malarial parasites, Pv, Pm and Po [130]. Thus, it is likely that an inhibitor of PfPM4 would reduce parasitic growth, regardless of the infecting species.

4.2. Tert-hydroxy- α -alkylnorstatine

In 2003, Nezami et al. reported a norstatine-based compound (KNI-10006, Fig. 26) that could inhibit all four plasmepsins in the DV of Pf at nanomolecular concentration ranges [131]. The IC₅₀ values for this PI against PfPM2 and PfPM4 were 39 nM and 15 nM, respectively, and the K_i value for PfPM2 was ca. 1 nM. However,

KNI-10006 was also active against human cathepsin D, with a K_i value of 2 nM and the compound had a low capacity for decreasing parasitic growth in Pf-infected erythrocyte cultures, with an IC₅₀ of 6.8 μ M, probably because of low cell or vacuole membrane permeation.

We used the tertiary alcohol TS-mimicking strategy to overcome these short-comings, and prepared *tert*-OH- α -alkylnorstatine-type inhibitors by varying the P1' pseudoresidue and changing the stereochemistry and the size of the P1 α -substituent [132]. The intermediate N-unsubstituted α -benzyl and α -phenylnorstatines were obtained by opening the rings of the respective diastereomerically pure epoxides 57 using aqueous ammonia. Subsequent condensation with the P2 group, 2-(2,6-dimethylphenoxy)acetic acid, gave the final stereopure inhibitors 58 (Fig. 27); each of the four diastereomers was isolated by high-performance liquid chromatography (HPLC) [132].

Fig. 27 shows the K_i values of tertiary alcohol α -phenylnorstatine PIs (S)-58 and (R)-58, which were obtained from the epoxides (S)-57 and (R)-57, respectively. These K_i values were used to evaluate the efficacy and selectivity for inhibiting the paralogous enzymes PfPM2 and PfPM4 and the orthologs of the latter, PmPM4, PoPM4 and PvPM4. When compared to KNI-10006, (S)-58 and (R)-58 were more than 4 orders of magnitude less potent, suggesting that the steric congestion obtained by altering the P1 side chain in the norstatine scaffold from the β -to the α -carbon was not suitable for the enzyme–inhibitor interaction. In general, the α -benzylnorstatines were less active than the α -phenylnorstatines. Compound (S)-58 was the most potent inhibitor of PoPM4, with a K_i value of 0.11 μ M and also had the best antiviral activity in the whole series for all the tested enzymes. The preferred P1' motif for all α -phenylnorstatines was L-Dmt, which was also incorporated into (S)-58. With regard to PvPM4, all inhibitors were active, with K_i values of 0.12–2.2 μ M.

4.3. Computational evaluation of the tert-hydroxy- α -alkylnorstatine TS-mimicking inhibitors

Fig. 28 shows the structures of the PfPM4 enzyme–inhibitor complexes, for inhibitors (R)-58 and (S)-58, as average coordinates of the molecular dynamics trajectories sampled for binding free energy calculations [132]. In inhibitor (R)-58, which has the same absolute configuration at P1' as KNI-10006, the binding pose was conserved. The α -hydroxy TS-mimicking group interacted with Asp34, whereas the adjacent P1 carbonyl group pointed in the opposite direction, interacting with Thr217 in the S1 subsite. In (S)-58, the carbonyl group at P1 pointed towards the tip of the flap and the carbonyl in P1' pointed towards the inner part of the enzyme, interacting with Thr217.

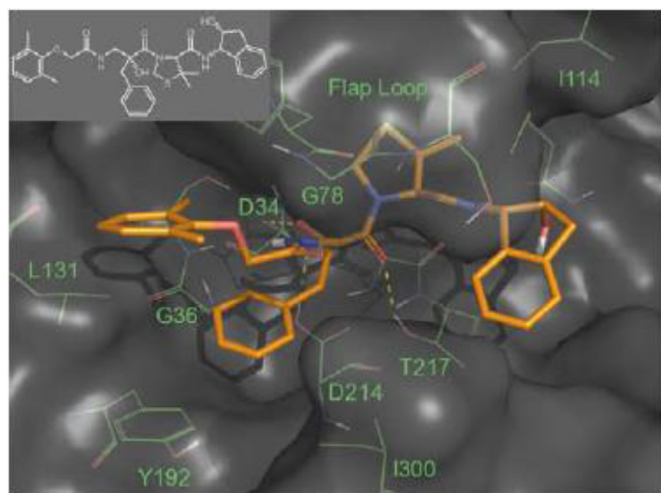
4.4. Prospects

Even though there are only small differences in the active sites of the four PM4 enzymes, studies on the *tert*-hydroxy- α -alkylnorstatine inhibitors showed certain variations in the respective inhibition activity dependable on the enzyme orthologue. The design and computational information of the tertiary alcohol TS mimicking inhibitors reported could provide assistance for improved design of new and more active PM4 inhibitors.

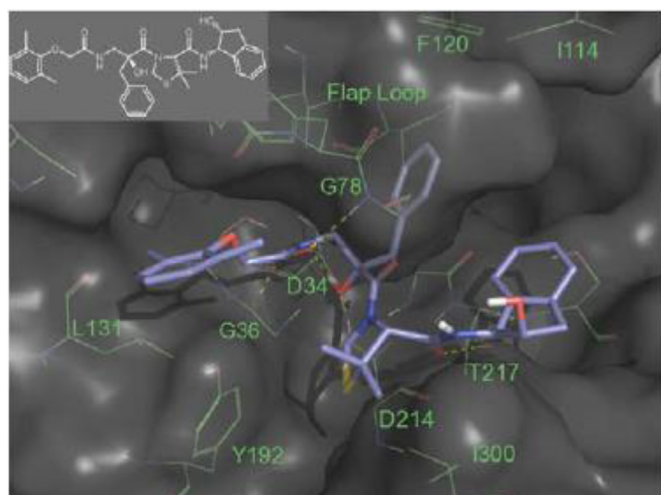
5. BACE-1 inhibitors

5.1. Background

AD is a common form of dementia among the elderly; worldwide ca. 35 million people currently live with the condition [133].

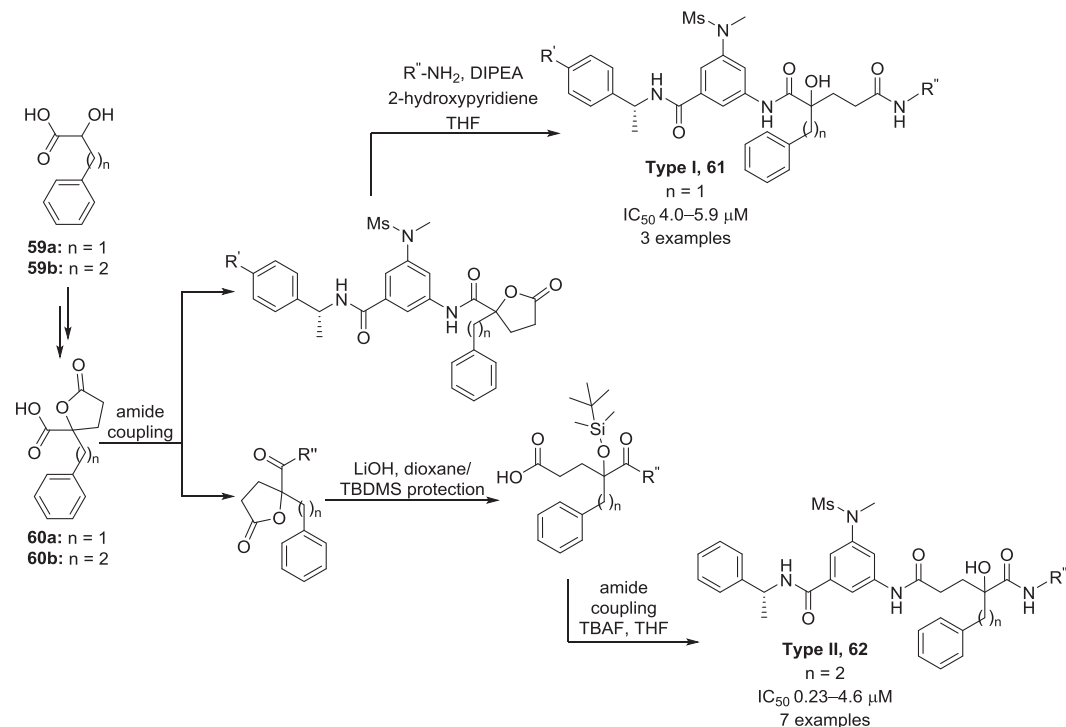


PfPM4 enzyme-inhibitor (R)-58 complex



PfPM4 enzyme-inhibitor (S)-58 complex

Fig. 28. Computer-generated PfPM4 enzyme–inhibitor binding modes, (R)-58 in orange and (S)-58 in purple. Hydrogen bonds are indicated by yellow dashed lines [132]. (For interpretation of the references to color in this figure legend, the reader is referred to the web version of this article.)

Synthesis of Type I and Type II inhibitorsBiological data of selected Type II inhibitors

Cmpd	R''	BACE-1 IC_{50} (μ M)	Cmpd	R''	BACE-1 IC_{50} (μ M)
62a-(A) ^a		0.57	62c-(A) ^{a,c,d}		0.23
62b-(B) ^{a,b}		0.25	62d-(B) ^{a,d}		0.32

^aCatD $K_i > 5000$ nM; ^b P_{app} (Caco-2) < 1×10^{-6} cm/s;
^c P_{app} (Caco-2) = 1.2×10^{-6} cm/s; ^dCatD was determined on a diastereomeric mixture (1:1).

Fig. 29. Chemistry and biological evaluation of the *tert*-hydroxystatin-like TS-mimicking BACE-1 inhibitors.

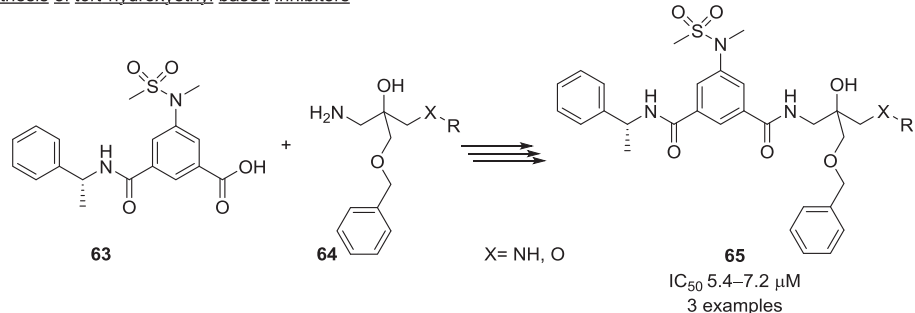
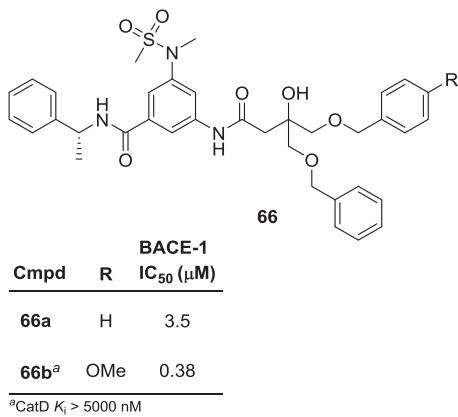
The diagnostic signs of AD include accumulation and extracellular aggregation of insoluble amyloid beta (A β) deposits (plaques) and intracellular neurofibrillary tangles in the brain. BACE-1 (β -secretase-1 or memapsin-2) processes the amyloid precursor protein during A β production [134]. Reduction of A β formation has long been associated with the human AP BACE-1 and the evaluation of this human enzyme as a therapeutic target has generated a lot of interest [135,136]. A study in BACE-1 knockout mice showed that A β was not produced, suggesting that AD can be influenced by the inhibition of BACE-1 [137,138].

Our earlier work on HIV-I PIs (discussed in Section 3) showed that inhibitors containing a shielded tertiary hydroxyl group as the TS mimic improved Caco-2 cell membrane permeation while retaining good viral inhibition. And so forth we became interested in developing BACE-1 inhibitors that contained a tertiary hydroxyl group as the central TS isostere. Below, we describe the various classes of BACE-1 inhibitors in the literature that have tertiary hydroxyl TS mimics.

5.2. *Tert*-hydroxystatin-like inhibitors

In 2009, our laboratory reported a series of *tert*-hydroxystatin-like BACE-1 inhibitors that had a benzyl or phenylethylene group in the P1 position [139]. Two tertiary statine-like moieties (denoted Type I and Type II, Fig. 29) were obtained; these were used with a substituted isophthalamide containing an inverted amide bond and variations at the P2'-P3' position, with the aim of binding to the S2'-S3' BACE-1 enzyme subsites.

Fig. 29 shows the synthesis of this class of inhibitors [139]. 2-Hydroxy-3-phenyl-propionic acid 59a (Type I) and 2-hydroxy-4-phenyl-butyric acid 59b (Type II) were treated stepwise; viz. protection, methyl acrylate alkylation of ketals and then intermolecular lactone formation. Compounds 60a-b were used as the common intermediates for Types I and II inhibitors in this class. Coupling the acid part with the selected amines, followed by ring opening, rendered Type I inhibitors 61. To obtain Type II inhibitors

Synthesis of *tert*-hydroxyethyl based inhibitorsBiological data of selected (inverted amide) inhibitors**Fig. 30.** Chemistry and biological evaluation of the *tert*-hydroxyethyl-based TS-mimicking BACE-1 inhibitors.

62, a series of reactions involving TBS protection, peptide coupling and deprotection was carried out.

The PIs synthesized were tested against BACE-1 and the IC₅₀ values were determined (Fig. 29) [139]. It soon became evident that the Type I tertiary TS mimics with modifications to a tertiary hydroxyl group on the same carbon as the presumed P1 substituent were not appropriate for the BACE-1 protease active site. This led us to the generic *tert*-hydroxystatin-like Type II inhibitors, with the central building block containing two available protected carboxylic acid functionalities that could be used orthogonally. This class of inhibitors had improved BACE-1 inhibition activity [139]. The activity after elongation at the P1-position to two carbons was ca. 10-fold better than for one carbon [139]. The best compounds in this series were **62b** and **62c** (IC₅₀ 0.25 and 0.23 μM, respectively). As the **62c** and **62d** epimers had similar potencies, it was assumed that the absolute stereochemistry at the quaternary center was less significant in the tertiary alcohol-shielded BACE-1 inhibitors. When the most potent inhibitors from the series were screened for inhibition of human cathepsin D, they were selective for BACE-1 (CatD K_i > 5000 nM). Caco-2 analysis for compounds **62b** and **62c** showed relatively poor membrane permeation ($P_{app} < 1 \times 10^{-6}$ and 1.2×10^{-6} cm/s, respectively), suggesting that this class of inhibitors requires further optimization to obtain acceptable pharmacokinetic properties.

5.3. *Tert*-hydroxyethylamine, *tert*-hydroxyethyl hydrazide (type II) and *tert*-hydroxyethylether

While we were exploring the potential of BACE-1 inhibitors containing tertiary alcohol TS mimics, we reported three more that closely resembled each other: *tert*-hydroxyethylamine, *tert*-

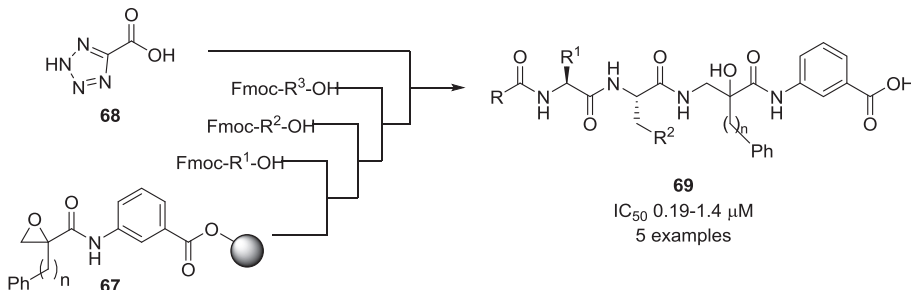
hydroxyethyl hydrazide (type II) and *tert*-hydroxyethylether [140]. This part of the work was inspired by previously prepared BACE-1 inhibitors containing *sec*-hydroxyethylamine isostere derivatives [137]. Inhibitors with the general structure of **65** containing tertiary alcohol TS mimics and prime side X-R chains were obtained by amide coupling of the non-prime building block **63** (5-substituted isophthalamic acid) with aminoalcohols **64** with different functional X-R groups (Fig. 30) [140]. However, significant BACE-1 inhibition was not obtained (IC₅₀ > 5.4 μM) for these compounds, even when various P1'-P2' groups were tested. This led us to synthesize and test compounds **66a** and **66b** with an inverted amide on the non-prime side. Compound **66b**, in which a *para*-methoxy group was incorporated as the P1' substituent, was the most potent BACE-1 inhibitor in this class (Fig. 30).

5.4. *Tert*-hydroxy- α -alkynorstatine (type I, triamide)

In the process of expanding the tertiary alcohol-containing BACE-1 inhibitors, we investigated the α -alkynorstatine (type I, triamide) TS mimic [141], and subsequently synthesized about 20 new inhibitors containing α -phenylnorstatine, α -benzylnorstatine, iso-serine and β -alanine moieties. The synthesis of these inhibitors based on fluorenylmethoxycarbonyl (Fmoc) solid-phase chemistry, and the biological evaluation and X-ray crystallography of the most active compounds co-crystallized with BACE-1 protease are described below.

Fig. 31 shows the final steps in the synthesis of the inhibitors containing an α -phenylnorstatine ($n = 1$) or α -benzylnorstatine ($n = 2$) TS mimic. Epoxides **67** were attached to a resin (2-chlorotriptyl chloride). Ammonia was used to open the epoxides **67**, which were diversified with various Fmoc-protected amino

Synthesis of α -phenylnorstatine ($n \equiv 1$) or α -benzylnorstatine ($n \equiv 2$)



Biological data of selected inhibitors

Cmpd	Structure	BACE-1 IC ₅₀ (μM)
69a		0.0082
(<i>R</i>)- 69b		0.19
69c		0.43

Fig. 31. Chemistry and biological evaluation of the *tert*-hydroxy- α -alkynorstatine TS-mimicking BACE-1 inhibitors.

acids using solid-phase chemistry. Next, tetrazole **68** was attached and the final compounds **69** were cleaved from the resin, followed by HPLC purification. The modification from the phenylnorstatine (*sec*-alcohol, **69a**) TS mimic to the α -phenylnorstatine (*tert*-alcohol)-containing core structure resulted in decreased inhibition potency, as seen with compounds **69a** (IC₅₀ 8.2 nM) and **69c** (epimeric 1:1 mixture, IC₅₀ 0.43 μM). Increasing the tether by one carbon (α -benzylnorstatine) gave a slightly more active inhibitor (**69b**). The respective diastereomers (*R*)-**69b** and (*S*)-**69b** had IC₅₀ values of 0.19 μM and 1.4 μM, respectively.

Two more series of BACE inhibitors, one containing *sec*-hydroxy TS mimics and one without the *tert*-alcohol and the aromatic tether, were synthesized to investigate the usefulness of the phenyl and benzyl groups; however, the PIs were comparatively less potent than the tertiary alcohol-based inhibitors. Further, starting from Fmoc-protected *iso*-serine and leucine, two more compounds with reduced C-terminals were synthesized; however, these were also less potent, with IC₅₀ values of 4–6 μM.

5.5. X-ray crystallography

Fig. 32 shows the X-ray crystallography structure (PDB code: 3KYR) of inhibitor (*R*)-**69b** co-crystallized with BACE-1 [141]. The hydrogen bond to Asp228 is from the N-terminal amine and not the *tert*-hydroxy. The tetrazole carbonyl (**Fig. 32 a**) of the inhibitor is close to Arg235 and there is a hydrogen bond between one of the nitrogens in the tetrazole and Tyr198. Further, there is an interaction between the N-terminal carbonyl in the inhibitor and the flap residue Thr72, while the Val-NH (**Fig. 32 b**) coordinates with Gly34 and the Val-carbonyl coordinates with Thr198. There is hydrogen bonding between Leu-NH (**Fig. 32 c**) and Pro70 (flap), and the Leu-carbonyl is in close proximity to Thr198. There are polar interactions between the C-terminal carboxylic functionality (**Fig. 32 e**) and Thr68 and Lys75, and hydrogen bonding between the carbonyl next to the *tert*-alcohol and Arg128. The inhibitor (*R*)-**69b** is locked in its arrangement by several internal interactions. The phenylethyl side chain (**Fig. 32 d**) of the α -benzylnorstatine isostere may not be essential for protein interaction as it is solvent-exposed and does not interact with the protein.

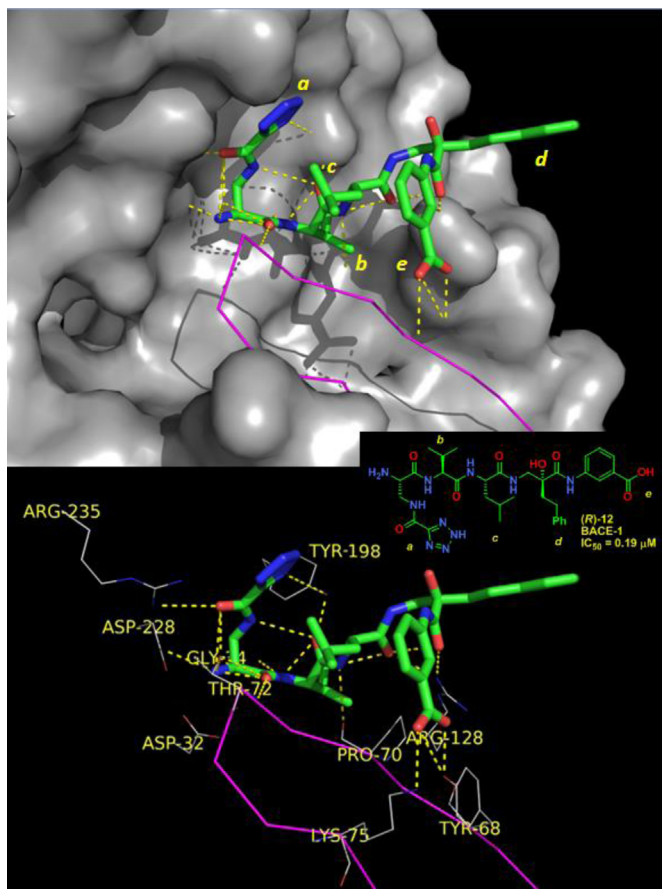


Fig. 32. X-ray crystallography structure of inhibitor (R)-69b (green) co-crystallized with BACE-1 [141]. (For interpretation of the references to color in this figure legend, the reader is referred to the web version of this article.)

5.6. Prospects

The BACE-1 inhibitors comprising a tertiary alcohol TS mimic that were synthesized and evaluated had moderate to low inhibition activity. The most potent PI synthesized was compound (R)-69b having an IC_{50} value of 0.19 μ M. A novel binding mode for the *tert*-alcohol containing α -alkynorstatine class of compounds was suggested by X-ray crystallography, where the N-terminal amine acted as the TS-isostere and not the *tert*-hydroxy group. These findings might be important for future drug discovery towards new BACE-1 inhibitors.

6. Conclusions and future directions

APs are validated drug targets. Further, the small size of the human AP family becomes an advantage when designing PIs that will target non-human APs from pathogenic viruses (such as HIV-1 protease) and parasites (such as the plasmepsins) because there will be less problems with selectivity. Since the 1980s when the first *tert*-hydroxy containing AP inhibitor was described, enormous progress has been achieved with a vast number of tertiary alcohol containing AP inhibitors reported. AP substrates have been successfully converted to linear and cyclic peptidomimetic inhibitors comprising a central tertiary hydroxyl group in the core structure. In this review, we structurally classified the *tert*-hydroxy TS mimics for APs inhibitors into ten different types. X-ray crystallography, computational structure-based design and synthesis of potent PIs with high selectivity, improved bioavailability and unique

resistance profile are summarized. Over the last decade, our group has provided a contribution in the development of HIV-1 PIs comprising *tert*-hydroxy TS analogs. Moreover, a significant effort has been directed towards extending the *tert*-hydroxy-based drug discovery strategy across the AP family. Although advancements have been made with regard to structural information and inhibitory activities of APs, there is still scope for improvement, particularly with metabolic stability, membrane permeability and *in vivo* toxicity.

Potent PIs against pepsin and HIV-1 protease have been developed with the *tert*-hydroxy substrate-based analogs mimicking the tetrahedral intermediate observed in the peptide cleavage mechanism. Inhibitor 50b, a *tert*-hydroxypropylhydrazide TS mimic, with K_i 1.7 nM and EC_{50} 7 nM against HIV-1 protease is proposed as one of the promising leads for improving the pharmaceutical characteristics. A macrocyclization strategy, as exemplified by compound 47b, is highlighted for further optimization to improve its pharmacokinetic profile.

In the future, additional studies will be necessary on the *tert*-hydroxy based strategy to advance the inhibitors into clinical trials. This review adds insights into the structural requirement for improvement of both enzymatic and cellular potency and cell permeability of AP inhibitors to be useful as therapeutic agents. We believe that with the advancement in studies of some of the TS mimics discussed in this review, novel marketed tertiary alcohol containing protease inhibitor(s) will not be too long away from now, thus providing alternative options for the treatment of various diseases.

Notes

The authors declare no competing financial interest.

Acknowledgment

We thank Uppsala University, Medivir AB and the Swedish Pharmaceutical Society for awarding Elisabeth och Alfred Ahlqvists stiftelse to HVM.

References

- [1] P.B. Szczesniak, The aspartic proteases, Scand. J. Clin. Lab. Investig. 52 (1992) 5–22.
- [2] D.R. Davies, The structure and function of the aspartic proteinases, Annu. Rev. Biophys. Bio. 19 (1990) 189–215.
- [3] J. Eder, U. Hommel, F. Cumin, B. Martoglio, B. Gerhartz, Aspartic proteases in drug discovery, Curr. Pharm. Des. 13 (2007) 271–285.
- [4] D.H. Rich, F.G. Salituro, M.W. Holladay, Conformationally directed drug design, in: J.A. Vida, M. Gordon (Eds.), ACS Symposium Series, vol. 251, 1984, pp. 213–237.
- [5] V.L. Schramm, Transition states, analogues, and drug development, ACS Chem. Biol. 8 (2013) 71–81.
- [6] D.B. Northrop, Follow the protons: a low-barrier hydrogen bond unifies the mechanisms of the aspartic proteases, Acc. Chem. Res. 34 (2001) 790–797.
- [7] B. Veerapandian, J.B. Cooper, A. Sali, T.L. Blundell, R.L. Rosati, B.W. Dominy, D.B. Damon, D.J. Hoover, Direct observation by X-ray-analysis of the tetrahedral intermediate of aspartic proteinases, Pro. Sci. 1 (1992) 322–328.
- [8] B.M. Dunn, Structure and mechanism of the pepsin-like family of aspartic peptidases, Chem. Rev. 102 (2002) 4431–4458.
- [9] I. Schechter, A. Berger, On the size of the active site in proteases. I. Papain, Biochem. Biophys. Res. Commun. 27 (1967) 157–162.
- [10] J. Rahuel, J.P. Priestle, M.G. Grutter, The crystal-structures of recombinant glycosylated human renin alone and in complex with a transition-state analog inhibitor, J. Struct. Biol. 107 (1991) 227–236.
- [11] M. Fujinaga, M.M. Chernaia, N.I. Tarasova, S.C. Mosimann, M.N.G. James, Crystal-structure of human pepsin and its complex with pepstatin, Prot. Sci. 4 (1995) 960–972.
- [12] P. Metcalf, M. Fusek, 2 crystal-structures for cathepsin-D – the lysosomal targeting signal and active-site, EMBO J. 12 (1993) 1293–1302.
- [13] N. Ostermann, B. Gerhartz, S. Worpenberg, J. Trappe, J. Eder, Crystal structure of an activation intermediate of cathepsin E, J. Mol. Biol. 342 (2004) 889–899.

- [14] H. Shimizu, A. Tosaki, K. Kaneko, T. Hisano, T. Sakurai, N. Nukina, Crystal structure of an active form of BACE1, an enzyme responsible for amyloid beta protein production, *Mol. Cell. Biol.* 28 (2008) 3663–3671.
- [15] V. Schauer-Vukasinovic, D. Bur, E. Kitas, D. Schlatter, G. Rosse, H.W. Lahm, T. Giller, Purification and characterization of active recombinant human napsin A, *Eur. J. Biochem.* 267 (2000) 2573–2580.
- [16] C. Dash, A. Kulkarni, B. Dunn, M. Rao, Aspartic peptidase inhibitors: implications in drug development, *Crit. Rev. Biochem. Mol. Biol.* 38 (2003) 89–119.
- [17] A. Brik, C.H. Wong, HIV-1 protease: mechanism and drug discovery, *Org. Biomol. Chem.* 1 (2003) 5–14.
- [18] H. Umezawa, T. Aoyagi, H. Morishim, M. Matsuzak, M. Hamada, T. Takeuchi, Pepstatin, a new pepsin inhibitor produced by actinomycetes, *J. Antibiot.* 23 (1970) 259–262.
- [19] I.A. Reid, B.J. Morris, W.F. Ganong, The renin-angiotensin system, *Annu. Rev. Physiol.* 40 (1978) 377–410.
- [20] J.M. Wood, J.L. Stanton, K.G. Hofbauer, *J. Enzyme Inhib. 1* (1987) 169–185.
- [21] H.M. Siragy, Renin inhibition: a new modality for hypertension management, *Curr. Hypertens. Rep.* 9 (2007) 291–294.
- [22] D.H. Rich, E.T.O. Sun, E. Ulm, Synthesis of analogs of the carboxyl protease inhibitor pepstatin – effect of structure on inhibition of pepsin and renin, *J. Med. Chem.* 23 (1980) 27–33.
- [23] J. Boger, N.S. Lohr, E.H. Ulm, M. Poe, E.H. Blaine, G.M. Fanelli, T.Y. Lin, L.S. Payne, T.W. Schorn, B.I. Lamont, T.C. Vassil, I.I. Stabilito, D.F. Veber, D.H. Rich, A.S. Bopari, Novel renin inhibitors containing the amino acid statine, *Nature* 303 (1983) 81–84.
- [24] M. Szelke, D.M. Jones, B. Atrash, A. Hallett, B. Leckie, Peptides: structure and function, in: F.J. Hruby, D.H. Rich (Eds.), *Proceedings of the Eighth American Peptide Symposium*, 1983, pp. 579–582.
- [25] D. Leung, G. Abbenante, D.P. Fairlie, Protease inhibitors: current status and future prospects, *J. Med. Chem.* 43 (2000) 305–341.
- [26] J.B. Cooper, Aspartic proteinases in disease: a structural perspective, *Curr. Drug Targets* 3 (2002) 155–173.
- [27] G. Zuccarello, A. Bouzide, I. Kvarnstrom, G. Niklasson, S.C.T. Svensson, M. Brisander, H. Danielsson, U. Nillroth, A. Karlen, A. Hallberg, B. Classon, B. Samuelsson, HIV-1 protease inhibitors based on acyclic carbohydrates, *J. Org. Chem.* 63 (1998) 4898–4906.
- [28] M. Alterman, M. Björnsne, A. Muhlman, B. Classon, I. Kvarnström, H. Danielson, P.O. Markgren, U. Nillroth, T. Unge, A. Hallberg, B. Samuelsson, Design and synthesis of new potent C-2-symmetric HIV-1 protease inhibitors. Use of L-mannaric acid as a peptidomimetic scaffold, *J. Med. Chem.* 41 (1998) 3782–3792.
- [29] M. Alterman, H.O. Andersson, N. Garg, G. Ahlsen, S. Lovgren, B. Classon, U.H. Danielson, I. Kvarnstrom, L. Vrang, T. Unge, B. Samuelsson, A. Hallberg, Design and fast synthesis of C-terminal duplicated potent C2-symmetric P1/P1'-modified HIV-1 protease inhibitors, *J. Med. Chem.* 42 (1999) 3835–3844.
- [30] J. Hultén, H.O. Andersson, W. Schaal, H.U. Danielson, B. Classon, I. Kvarnstrom, A. Karlen, T. Unge, B. Samuelsson, A. Hallberg, Inhibitors of the C-2-symmetric HIV-1 protease: nonsymmetric binding of a symmetric cyclic sulfamide with ketoxime groups in the P2/P2' side chains, *J. Med. Chem.* 42 (1999) 4054–4061.
- [31] J. Wachtmeister, A. Muhlman, B. Classon, I. Kvarnstrom, A. Hallberg, B. Samuelsson, Impact of the central hydroxyl groups on the activity of symmetrical HIV-1 protease inhibitors derived from L-mannaric acid, *Tetrahedron* 56 (2000) 3219–3225.
- [32] K. Oscarsson, B. Classon, I. Kvarnstrom, A. Hallberg, B. Samuelsson, Solid phase assisted synthesis of HIV-1 protease inhibitors. Expedient entry to unsymmetrical substitution of a C-2 symmetric template, *Can. J. Chem.* 78 (2000) 829–837.
- [33] M. Alterman, *Design and Synthesis of HIV-1 Protease Inhibitors*, Uppsala University, 2001, pp. 1–70.
- [34] D. Pyring, L. Lindberg, A. Rosenquist, G. Zuccarello, I. Kvarnstrom, H. Zhang, L. Vrang, T. Unge, B. Classon, A. Hallberg, B. Samuelsson, Design and synthesis of potent C-2-symmetric diol-based HIV-1 protease inhibitors: effects of fluoro substitution, *J. Med. Chem.* 44 (2001) 3083–3091.
- [35] A. Muhlman, B. Classon, A. Hallberg, B. Samuelsson, Synthesis of potent C-2-symmetric, diol-based HIV-1 protease inhibitors. Investigation of thioalkyl and thioaryl P1/P1' substituents, *J. Med. Chem.* 44 (2001) 3402–3406.
- [36] K. Oscarsson, M. Lahmann, J. Lindberg, J. Kangasmetsa, T. Unge, S. Oscarson, A. Hallberg, B. Samuelsson, Design and synthesis of HIV-1 protease inhibitors. Novel tetrahydrafuran P2/P2'-groups interacting with Asp29/30 of the HIV-1 protease. Determination of binding from X-ray crystal structure of inhibitor protease complex, *Bioorg. Med. Chem.* 11 (2003) 1107–1115.
- [37] H.O. Andersson, K. Fridborg, S. Lövgren, M. Alterman, A. Muhlman, M. Björnsne, N. Garg, I. Kvarnström, W. Schaal, B. Classon, A. Karlen, U.H. Danielsson, G. Ahlsen, U. Nillroth, L. Vrang, B. Oberg, B. Samuelsson, A. Hallberg, T. Unge, Optimization of P1-P3 groups in symmetric and asymmetric HIV-1 protease inhibitors, *Eur. J. Biochem.* 270 (2003) 1746–1758.
- [38] J.K. Ekegren, T. Unge, M.Z. Safa, H. Wallberg, B. Samuelsson, A. Hallberg, A new class of HIV-1 protease inhibitors containing a tertiary alcohol in the transition-state mimicking scaffold, *J. Med. Chem.* 48 (2005) 8098–8102.
- [39] J. Wannberg, N.F.K. Kaiser, L. Vrang, B. Samuelsson, M. Larhed, A. Hallberg, High-speed synthesis of potent C₂-symmetric HIV-1 protease inhibitors by in-situ aminocarbonylations, *J. Comb. Chem.* 7 (2005) 611–617.
- [40] J.K. Ekegren, J. Gising, H. Wallberg, M. Larhed, B. Samuelsson, A. Hallberg, Variations of the P2 group in HIV-1 protease inhibitors containing a tertiary alcohol in the transition-state mimicking scaffold, *Org. Biomol. Chem.* 4 (2006) 3040–3043.
- [41] J.K. Ekegren, N. Ginman, A. Johansson, H. Wallberg, M. Larhed, B. Samuelsson, T. Unge, A. Hallberg, Microwave-accelerated synthesis of P1'-extended HIV-1 protease inhibitors encompassing a tertiary alcohol in the transition-state mimicking scaffold, *J. Med. Chem.* 49 (2006) 1828–1832.
- [42] J. Wannberg, Y.A. Sábnis, L. Vrang, B. Samuelsson, A. Karlen, A. Hallberg, M. Larhed, A new structural theme in C₂-symmetric HIV-1 protease inhibitors: ortho-substituted P1/P1' side chains, *Bioorg. Med. Chem.* 14 (2006) 5303–5315.
- [43] X.Y. Wu, P. Ohrngren, J.K. Ekegren, J. Unge, T. Unge, H. Wallberg, B. Samuelsson, A. Hallberg, M. Larhed, Two-carbon-elongated HIV-1 protease inhibitors with a tertiary-alcohol-containing transition-state mimic, *J. Med. Chem.* 51 (2008) 1053–1057.
- [44] A.K. Mahalingam, L. Axelsson, J.K. Ekegren, J. Wannberg, J. Kihlstrom, T. Unge, H. Wallberg, B. Samuelsson, M. Larhed, A. Hallberg, HIV-1 protease inhibitors with a transition-state mimic comprising a tertiary alcohol: improved anti-viral activity in cells, *J. Med. Chem.* 53 (2010) 607–615.
- [45] P. Ohrngren, X.Y. Wu, M. Persson, J.K. Ekegren, H. Wallberg, L. Vrang, A. Rosenquist, B. Samuelsson, T. Unge, M. Larhed, HIV-1 protease inhibitors with a tertiary alcohol containing transition-state mimic and various P2 and P1' substituents, *Med. Chem. Comm.* 2 (2011) 701–709.
- [46] X. Wu, P. Ohrngren, A. Joshi, A. Trejos, M. Persson, R.K. Arvela, H. Wallberg, L. Vrang, A. Rosenquist, B. Samuelsson, T. Unge, M. Larhed, Synthesis, X-ray analysis, and biological evaluation of a new class of stereopure lactam-based HIV-1 protease inhibitors, *J. Med. Chem.* 55 (2012) 2724–2736.
- [47] P.Y.S. Lam, P.K. Jadhav, C.J. Eyermann, C.N. Hodge, Y. Ru, L.T. Bacheler, O.M.J. Meek, M. Rayner, Rational design of potent, bioavailable, nonpeptide cyclic ureas as HIV protease inhibitors, *Science* 263 (1994) 380–384.
- [48] J. Hultén, N.M. Bonham, U. Nillroth, T. Hansson, G. Zuccarello, A. Bouzide, J. Aqvist, B. Classon, U.H. Danielson, A. Karlen, I. Kvarnstrom, B. Samuelsson, A. Hallberg, Cyclic HIV-1 protease inhibitors derived from mannitol: synthesis, inhibitory potencies, and computational predictions of binding affinities, *J. Med. Chem.* 40 (1997) 885–897.
- [49] A. Ax, A.A. Joshi, K.M. Orrling, L. Vrang, B. Samuelsson, A. Hallberg, A. Karlen, M. Larhed, Synthesis of a small library of non-symmetric cyclic sulfamide HIV-1 protease inhibitors, *Tetrahedron* 66 (2010) 4049–4056.
- [50] A. Ax, W. Schaaf, L. Vrang, B. Samuelsson, A. Hallberg, A. Karlen, M. Larhed, Cyclic sulfamide HIV-1 protease inhibitors, with sidechains spanning from P2/P2' to P1/P1', *Bioorg. Med. Chem.* 13 (2005) 755–764.
- [51] A. Joshi, J.B. Veron, J. Unge, A. Rosenquist, H. Wallberg, B. Samuelsson, A. Hallberg, M. Larhed, Design and synthesis of P1-P3 macrocyclic tertiary-alcohol-comprising HIV-1 protease inhibitors, *J. Med. Chem.* 56 (2013) 8999–9007.
- [52] K. Ersmark, I. Feierberg, S. Bjelic, J. Hultén, B. Samuelsson, J. Aqvist, A. Hallberg, Synthesis, biological evaluation, and molecular docking studies of novel 1,3,4-oxadiazole derivatives possessing benzotriazole moiety as FAK inhibitors with anticancer activity, *Bioorg. Med. Chem.* 11 (2003) 3723–3729.
- [53] J. Marelius, M. Graffner-Nordberg, T. Hansson, A. Hallberg, J. Aqvist, Computation of affinity and selectivity: binding of 2,4-diaminopteridine and 2,4-diaminoquinazoline inhibitors to dihydrofolate reductases, *J. Comput. Aided Mol. Des.* 12 (1998) 119–131.
- [54] M. Graffner-Nordberg, J. Marelius, S. Ohlsson, A. Persson, G. Swedberg, P. Andersson, S.E. Andersson, J. Aqvist, A. Hallberg, Computational predictions of binding affinities to dihydrofolate reductase: synthesis and biological evaluation of methotrexate analogues, *J. Med. Chem.* 43 (2000) 3852–3861.
- [55] P. Artursson, K. Palm, K. Luthman, Caco-2 monolayers in experimental and theoretical predictions of drug transport, *Adv. Drug Deliv. Rev.* 46 (2001) 27–43.
- [56] R.A. Conradi, A.R. Hilgers, N.F. Ho, P.S. Burton, The influence of peptide structure on transport across Caco-2 cells. II. Peptide bond modification which results in improved permeability, *Pharm. Res.* 9 (1992) 435–439.
- [57] D.C. Kim, P.S. Burton, R.T. Borchardt, A correlation between the permeability characteristics of a series of peptides using an *in vitro* cell culture model (Caco-2) and those using an *in situ* perfused rat ileum model of the intestinal mucosa, *Pharm. Res.* 10 (1993) 1710–1714.
- [58] M.A. Roseman, Hydrophobicity of the peptide C=O···H–N hydrogen-bonded group, *J. Mol. Biol.* 201 (1988) 621–623.
- [59] R.A. Conradi, A.R. Hilgers, P.S. Burton, J.B. Hester, Epithelial cell permeability of a series of peptidic HIV protease inhibitors: aminoterminal substituent effects, *J. Drug Target* 2 (1994) 167–171.
- [60] V.A. Ashwood, M.J. Field, D.C. Horwell, C. Julien-Larose, R.A. Lewthwaite, S. McCleary, M.C. Pritchard, J. Raphy, L. Singh, Utilization of an intramolecular hydrogen bond to increase the CNS penetration of an NK(1) receptor antagonist, *J. Med. Chem.* 44 (2001) 2276–2285.
- [61] J. Tang, R.N.S. Wong, Evolution in the structure and function of aspartic proteases, *J. Cell. Biochem.* 33 (1987) 53–63.
- [62] V. Cavailles, P. Augereau, H. Rochefort, Cathepsin D gene is controlled by a mixed promoter, and estrogens stimulate only TATA-dependent transcription in breast cancer cells, *Proc. Natl. Acad. Sci. U. S. A.* 90 (1993) 203–207.

- [63] T. Hofmann, R.S. Hodges, A new chromophoric substrate for penicillopepsin and other fungal aspartic proteinases, *Biochem. J.* 203 (1982) 603–610.
- [64] F.G. Salituro, N. Agarwal, T. Hofmann, D.H. Rich, Inhibition of aspartic proteinases by peptides containing lysine and ornithine side-chain analogues of statine, *J. Med. Chem.* 30 (1987) 286–295.
- [65] G. Mains, M. Takahashi, J. Sodek, T. Hofmann, The specificity of penicillopepsin, *Can. J. Biochem.* 49 (1971) 1134–1149.
- [66] M.N.G. James, A. Sielecki, F. Salituro, D.H. Rich, T. Hofmann, Conformational flexibility in the active sites of aspartyl proteinases revealed by a pepstatin fragment binding to penicillopepsin, *Proc. Natl. Acad. Sci. U. S. A.* 79 (1982) 6137–6141.
- [67] D.H. Rich, Pepstatin-derived inhibitors of aspartic proteinases. A close look at an apparent transition-state analogue inhibitor, *J. Med. Chem.* 28 (1985) 263–273.
- [68] D.H. Rich, M.S. Bernatowicz, N.S. Agarwal, M. Kawai, F.G. Salituro, P.G. Schmidt, Inhibition of aspartic proteases by pepstatin and 3-methylstatine derivatives of pepstatin. Evidence for collected-substrate enzyme inhibition, *Biochemistry* 24 (1985) 3165–3173.
- [69] M. Kawai, A.S. Boparai, M.S. Bernatowicz, D.H. Rich, Synthesis of novel 3-methylstatine analogs. Assignment of absolute configuration, *J. Org. Chem.* 48 (1983) 1876–1879.
- [70] S. Wain-Hobson, P. Sonigo, O. Danos, S. Cole, M. Alizon, Nucleotide sequence of the AIDS virus, LAV, *Cell* 40 (1985) 9–17.
- [71] M.A. Navia, P.M. Fitzgerald, B.M. McKeever, C.T. Leu, J.C. Heimbach, W.K. Herber, I.S. Sigal, P.L. Darke, J.P. Springer, Three-dimensional structure of aspartyl protease from human immunodeficiency virus HIV-1, *Nature* 337 (1989) 615–620.
- [72] A. Wlodawer, J.W. Erickson, Structure-based inhibitors of HIV-1 protease, *Annu. Rev. Biochem.* 62 (1993) 543–585.
- [73] M. Prabu-Jeyabalan, E. Nalivaika, C.A. Schiffer, Substrate shape determines specificity of recognition for HIV-1 protease: analysis of crystal structures of six substrate complexes, *Structure* 10 (2002) 369–381.
- [74] M. Miller, J. Schneider, B.K. Sathyaranayana, M.V. Toth, G.R. Marshall, L. Clawson, L. Selk, S.B.H. Kent, A. Wlodawer, Structure of complex of synthetic HIV-1 protease with a substrate-based inhibitor at 2.3 Å resolution, *Science* 246 (1989) 1149–1152.
- [75] A. Wlodawer, M. Miller, M. Jaskolski, B.K. Sathyaranayana, E. Baldwin, I.T. Weber, L.M. Selk, L. Clawson, J. Schneider, S.B.H. Kent, Conserved folding in retroviral proteases: crystal structure of a synthetic HIV-1 protease, *Science* 245 (1989) 616–621.
- [76] R. Lapatto, T. Blundell, A. Hemmings, J. Overington, A. Wilderspin, S. Wood, J.R. Merson, P.J. Whittle, D.E. Danley, K.F. Geoghegan, X-ray analysis of HIV-1 protease at 2.7 Å resolution confirms structural homology among retroviral enzymes, *Nature* 342 (1989) 299–302.
- [77] N.A. Roberts, J.A. Martin, D. Kinchington, A.V. Broadhurst, J.C. Craig, I.B. Duncan, S.A. Galpin, B.K. Handa, J. Kay, A. Krohn, R.W. Lambert, J.H. Merrett, J.S. Mills, K.E.B. Parkes, S. Redshaw, A.J. Ritchie, D.L. Taylor, G.J. Thomas, P.J. Machin, Rational design of peptide-based HIV proteinase inhibitors, *Science* 248 (1990) 358–361.
- [78] D.J. Kempf, K.C. Marsh, J.F. Denissen, E. McDonald, S. Vasavanonda, C.A. Flentge, B.E. Green, L. Fino, C.H. Park, X.P. Kong, N.E. Wideburg, A. Saldivar, L. Ruiz, W.M. Kati, H.L. Sham, T. Robins, K.D. Stewart, A. Hsu, J.J. Plattner, J.M. Leonard, D.W. Norbeck, ABT-538 is a potent inhibitor of human immunodeficiency virus protease and has high oral bioavailability in humans, *Proc. Natl. Acad. Sci. U. S. A.* 92 (1995) 2484–2488.
- [79] B.D. Dorsey, R.B. Levin, S.L. McDaniel, J.P. Vacca, J.P. Guare, P.L. Darke, J.A. Zugay, E.A. Emini, W.A. Schleif, J.C. Quintero, J.H. Lin, I.W. Chen, M.K. Holloway, P.M.D. Fitzgerald, M.G. Axel, D. Ostovic, P.S. Anderson, J.R. Huff, L-735,524: the design of a potent and orally bioavailable HIV protease inhibitor, *J. Med. Chem.* 37 (1994) 3443–3451.
- [80] A.K. Patick, H. Mo, M. Markowitz, K. Appelt, B. Wu, L. Musick, V. Kalish, S. Kaldor, S. Reich, D. Ho, S. Webber, Antiviral and resistance studies of AG1343, an orally bioavailable inhibitor of human immunodeficiency virus protease, *Antimicrob. Agents Chemother.* 40 (1996) 1575.
- [81] A. Mastrolorenzo, S. Rusconi, A. Scozzafava, G. Barbaro, C.T. Supuran, Inhibitors of HIV-1 protease: current state of the art 10 years after their introduction. From antiretroviral drugs to antifungal, antibacterial and antitumor agents based on aspartic protease inhibitors, *Curr. Med. Chem.* 14 (2007) 2734–2748.
- [82] T. Hawkins, Understanding and managing the adverse effects of antiretroviral therapy, *Antivir. Res.* 85 (2010) 201–209.
- [83] X.L.Z. Pang, G. Zhai, Advances in non-peptidomimetic HIV protease inhibitors, *Curr. Med. Chem.* 21 (2014) 1997–2011.
- [84] G.N. Kumar, A.D. Rodrigues, A.M. Buko, J.F. Denissen, Cytochrome P450-mediated metabolism of the HIV-1 protease inhibitor ritonavir (ABT-538) in human liver microsomes, *J. Pharmacol. Exp. Ther.* 277 (1996) 423–431.
- [85] F. Clavel, A.J. Hance, HIV drug resistance, *N. Engl. J. Med.* 350 (2004) 1023–1035.
- [86] L. Menéndez-Arias, Targeting HIV: antiretroviral therapy and development of drug resistance, *Trends Pharmacol. Sci.* 23 (2002) 381–388.
- [87] E.J. Corey, A. Guzman-Perez, The catalytic enantioselective construction of molecules with quaternary carbon stereocenters, *Angew. Chem. Int. Ed.* 37 (1998) 388–401.
- [88] X. Liu, E. Hu, X. Tian, A. Mazur, F.H. Ebetino, Enantioselective synthesis of phosphinyl peptidomimetics via an asymmetric Michael reaction of phosphinic acids with acrylate derivatives, *J. Organomet. Chem.* 646 (2002) 212–222.
- [89] G. Bold, A. Fässler, H.G. Capraro, R. Cozens, T. Klimkait, J. Lazzins, J. Mestan, B. Poncioni, J. Rösel, D. Stover, M. Tintelnot-Blomley, F. Acemoglu, W. Beck, E. Boss, M. Eschbach, T. Hurlmann, E. Masso, S. Roussel, K. Ucci-Stoll, D. Wyss, M. Lang, New aza-dipeptide analogues as potent and orally absorbed HIV-1 protease inhibitors: candidates for clinical development, *J. Med. Chem.* 41 (1998) 3387–3401.
- [90] J.H. Lin, Role of pharmacokinetics in the discovery and development of indinavir, *Adv. Drug Deliv. Rev.* 39 (1999) 33–49.
- [91] S.K. Balani, B.H. Arison, L. Mathai, L.R. Kauffman, R.R. Miller, R.A. Stearns, I.W. Chen, J.H. Lin, Metabolites of L-735,524, a potent HIV-1 protease inhibitor, in human urine, *Drug Metab. Dispos.* 23 (1995) 266–270.
- [92] M. Larhed, C. Moberg, A. Hallberg, Microwave-accelerated homogeneous catalysis in organic chemistry, *Acc. Chem. Res.* 35 (2002) 717–727.
- [93] M. Larhed, J. Wannberg, A. Hallberg, Controlled microwave heating as an enabling technology: expedient synthesis of protease inhibitors in perspective, *QSAR Comb. Sci.* 26 (2007) 51–68.
- [94] J. Gising, L.R. Odell, M. Larhed, Microwave-assisted synthesis of small molecules targeting the infectious diseases tuberculosis, HIV/AIDS, malaria and hepatitis C, *Org. Biomol. Chem.* 10 (2012) 2713–2729.
- [95] M. Larhed, G. Lindeberg, A. Hallberg, Rapid microwave-assisted Suzuki coupling on solid-phase, *Tetrahedron Lett.* 37 (1996) 8219–8222.
- [96] J.F. Miller, C.W. Andrews, M. Brieger, E.S. Furhne, M.R. Hale, M.H. Hanlon, R.J. Hazen, I. Kaldor, E.W. McLean, D. Reynolds, D.M. Sammond, A. Spaltenstein, R. Tung, E.M. Turner, X.R. Xu, R.G. Sherrill, Ultra-potent P1 modified arylsulfonamide HIV protease inhibitors: the discovery of GW0385, *Bioorg. Med. Chem. Lett.* 16 (2006) 1788–1794.
- [97] A. Fässler, G. Bold, H.G. Capraro, R. Cozens, J. Mestan, B. Poncioni, J. Rösel, M. Tintelnot-Blomley, M. Lang, Aza-peptide analogues as potent human immunodeficiency virus type-1 protease inhibitors with oral bioavailability, *J. Med. Chem.* 39 (1996) 3203–3216.
- [98] M.F. Wempe, P.L. Anderson, Atazanavir metabolism according to CYP3A5 status: an in vitro-in vivo assessment, *Drug Metab. Dispos.* 39 (2011) 522–527.
- [99] E. Marsault, M.L. Peterson, Macrocycles are great cycles: applications, opportunities, and challenges of synthetic macrocycles in drug discovery, *J. Med. Chem.* 54 (2011) 1961–2004.
- [100] R. Colombo, R. Rose, C. McLaren, A. Thiry, N. Parkin, J. Friberg, Identification of ISOL as the signature atazanavir (ATV)-resistance mutation in treatment-naïve HIV-1-infected patients receiving ATV-containing regimens, *J. Infect. Dis.* 189 (2004) 1802–1810.
- [101] T. Rezai, B. Yu, G.L. Millhauser, M.P. Jacobson, R.S. Lokey, Testing the conformational hypothesis of passive membrane permeability using synthetic cyclic peptide diastereomers, *J. Am. Chem. Soc.* 128 (2006) 2510–2511.
- [102] B.L. Podlogar, R.A. Farr, D. Friedrich, C. Tarnus, E.W. Huber, R.J. Cregge, D. Schirlin, Design, synthesis, and conformational-analysis of a novel macrocyclic HIV-protease inhibitor, *J. Med. Chem.* 37 (1994) 3684–3692.
- [103] Y. Tojo, Y. Koh, M. Amano, M. Aoki, D. Das, S. Kulkarni, D.D. Anderson, A.K. Ghosh, H. Mitsuya, Novel protease inhibitors (Pls) containing macrocyclic components and 3(R),3a(S),6a(R)-bis-tetrahydrofuranylurethane that are potent against multi-PI-resistant HIV-1 variants in vitro, *Antimicrob. Agents Chemother.* 54 (2010) 3460–3470.
- [104] D. Nöteberg, W. Schaaf, E. Hamelink, L. Vrang, M. Larhed, High-speed optimization of inhibitors of the malarial proteases plasmeprin I and II, *J. Comb. Chem.* 5 (2003) 456–464.
- [105] M. Larhed, M. Hoshino, S. Hadida, D.P. Curran, A. Hallberg, Rapid fluorous stille coupling reactions conducted under microwave irradiation, *J. Org. Chem.* 62 (1997) 5583–5587.
- [106] Y. Coquerel, J. Rodriguez, Microwave-assisted olefin metathesis, *Eur. J. Org. Chem.* (2008) 1125–1132.
- [107] M. De Rosa, J. Unge, H.V. Motwani, Å. Rosenquist, L. Vrang, H. Wallberg, M. Larhed, Macrocyclic transition-state mimicking HIV-1 protease inhibitors encompassing a tertiary alcohol, *J. Med. Chem.* 57 (2014) 6444–6457.
- [108] E.I. Negishi, Fundamental Properties of Palladium and Patterns of the Reactions of Palladium and Complexes, in: *Handbook of Organopalladium Chemistry for Organic Synthesis*, vol. 1, 2002, pp. 17–35.
- [109] M. Larhed, A. Hallberg, Microwave-promoted palladium-catalyzed coupling reactions, *J. Org. Chem.* 61 (1996) 9582–9584.
- [110] C.O. Kappe, D. Dallinger, The impact of microwave synthesis on drug discovery, *Nat. Rev. Drug Discov.* 5 (2006) 51–63.
- [111] C.S. Callam, T.L. Lowary, Suzuki cross-coupling reactions: synthesis of unsymmetrical biaryls in the organic laboratory, *J. Chem. Educ.* 78 (2001) 947–948.
- [112] N. Miyaura, A. Suzuki, Palladium-catalyzed cross-coupling reactions of organoboron compounds, *Chem. Rev.* 95 (1995) 2457–2483.
- [113] K. Billingsley, S.L. Buchwald, Highly efficient monophosphine-based catalyst for the palladium-catalyzed Suzuki–Miyaura reaction of heteroaryl halides and heteroaryl boronic acids and esters, *J. Am. Chem. Soc.* 129 (2007) 3358–3366.
- [114] E. Tyrrell, P. Brookes, The synthesis and applications of heterocyclic boronic acids, *Synthesis-Stuttgart* (2003) 469–483.

- [115] H. Clavier, C.A. Urbina-Blanco, S.P. Nolan, Indenyldene ruthenium complex bearing a sterically demanding NHC ligand: an efficient catalyst for olefin metathesis at room temperature, *Organometallics* 28 (2009) 2848–2854.
- [116] D. Rix, F. Cajio, I. Laurent, F. Boeda, H. Clavier, S.P. Nolan, M. Mauduit, Aminocarbonyl group containing Hoveyda-Grubbs-type complexes: synthesis and activity in olefin metathesis transformations, *J. Org. Chem.* 73 (2008) 4225–4228.
- [117] F.C. Courchay, J.C. Sworen, I. Chiviriga, K.A. Abboud, K.B. Wagener, Understanding structural isomerization during ruthenium-catalyzed olefin metathesis: a deuterium labeling study, *Organometallics* 25 (2006) 6074–6086.
- [118] B. Schmidt, An olefin metathesis/double bond isomerization sequence catalyzed by an *in situ* generated ruthenium hydride species, *Eur. J. Org. Chem.* (2003) 816–819.
- [119] A. Furstner, O.R. Thiel, L. Ackermann, H.J. Schanz, S.P. Nolan, Ruthenium carbene complexes with N,N'-bis(mesityl)imidazol-2-ylidene ligands: RCM catalysts of extended scope, *J. Org. Chem.* 65 (2000) 2204–2207.
- [120] C. de Mendoza, V. Soriano, Resistance to HIV protease inhibitors: mechanisms and clinical consequences, *Curr. Drug Metab.* 5 (2004) 321–328.
- [121] C. Armbruster, HIV-1 infection: recent developments in treatment and current management strategies, *Anti-Infect. Agents Med. Chem. (Formerly Curr. Med. Chem. Anti-Infect. Agents)* 7 (2008) 201–214.
- [122] World Malaria Report, World Health Organisation, Geneva, 2013, pp. 1–255.
- [123] M.S. Alilio, I.C. Bygbjerg, J.G. Breman, Are multilateral malaria research and control programs the most successful? Lessons from the past 100 years in Africa, *Am. J. Trop. Med. Hyg.* 71 (2004) 268–278.
- [124] A. Cohen, A. Dumetre, N. Azas, A decade of *Plasmodium falciparum* metabolic pathways of therapeutic interest to develop new selective antimalarial drugs, *Mini-Rev. Med. Chem.* 13 (2013) 1340–1347.
- [125] D.E. Neafsey, *Nat. Genet.* 45 (2013) 589–590.
- [126] K.G. Le Roch, D.W.D. Chung, N. Ponts, Genomics and integrated systems biology in *Plasmodium falciparum*: a path to malaria control and eradication, *Parasite Immunol.* 34 (2012) 50–60.
- [127] J.B. Dame, G.R. Reddy, C.A. Yowell, B.M. Dunn, J. Kay, C. Berry, Sequence, expression and modeled structure of an aspartic proteinase from the human malaria parasite *Plasmodium falciparum*, *Mol. Biochem. Parasitol.* 64 (1994) 177–190.
- [128] L. Tyas, I. Gluzman, R.P. Moon, K. Rupp, J. Westling, R.G. Ridley, J. Kay, D.E. Goldberg, C. Berry, Naturally-occurring and recombinant forms of the aspartic proteinases plasmepsins I and II from the human malaria parasite *Plasmodium falciparum*, *FEBS Lett.* 454 (1999) 210–214.
- [129] R. Banerjee, J. Liu, W. Beatty, L. Pelosof, M. Klemba, D.E. Goldberg, Four plasmepsins are active in the *Plasmodium falciparum* food vacuole, including a protease with an active-site histidine, *Proc. Natl. Acad. Sci. U. S. A.* 99 (2002) 990–995.
- [130] J.B. Dame, C.A. Yowell, L. Omara-Opyene, J.M. Carlton, R.A. Cooper, T. Li, Plasmepsin 4, the food vacuole aspartic proteinase found in all *Plasmodium* spp. infecting man, *Mol. Biochem. Parasitol.* 130 (2003) 1–12.
- [131] A. Nezami, T. Kimura, K. Hidaka, A. Kiso, J. Liu, Y. Kiso, D.E. Goldberg, E. Freire, High-affinity inhibition of a family of *Plasmodium falciparum* proteinases by a designed adaptive inhibitor, *Biochemistry* 42 (2003) 8459–8464.
- [132] K.M. Orrling, M.R. Marzahn, H. Gutierrez-de-Teran, J. Aqvist, B.M. Dunn, M. Larhed, α -Substituted norstatines as the transition-state mimic in inhibitors of multiple digestive vacuole malaria aspartic proteinases, *Bioorg. Med. Chem.* 17 (2009) 5933–5949.
- [133] World Alzheimer Report, Journey of Caring: an Analysis of Long-term Care for Dementia, Alzheimer's Disease International, 2013, pp. 1–88.
- [134] A.K. Ghosh, S. Gemma, J. Tang, β -Secretase as a therapeutic target for Alzheimer's disease, *Neurotherapeutics* 5 (2008) 399–408.
- [135] S.L. Cole, R. Vassar, BACE1 structure and function in health and Alzheimer's disease, *Curr. Alzheimer Res.* 5 (2008) 100–120.
- [136] S.L. Cole, R. Vassar, The role of amyloid precursor protein processing by BACE1, the beta-secretase, in Alzheimer disease pathophysiology, *J. Biol. Chem.* 283 (2008) 29621–29625.
- [137] R. Silvestri, Boom in the development of non-peptidic beta-secretase (BACE1) inhibitors for the treatment of Alzheimer's disease, *Med. Res. Rev.* 29 (2009) 295–338.
- [138] S.S. Sisodia, P.H. St George-Hyslop, γ -Secretase, notch, A β and Alzheimer's disease: where do the presenilins fit in? *Nat. Rev. Neurosci.* 3 (2002) 281–290.
- [139] F. Wangsell, F. Russo, J. Savmarker, A. Rosenquist, B. Samuelsson, M. Larhed, Design and synthesis of BACE-1 inhibitors utilizing a tertiary hydroxyl motif as the transition state mimic, *Bioorg. Med. Chem. Lett.* 19 (2009) 4711–4714.
- [140] F. Russo, F. Wangsell, J. Savmarker, M. Jacobsson, M. Larhed, Synthesis and evaluation of a new class of tertiary alcohol based BACE-1 inhibitors, *Tetrahedron* 65 (2009) 10047–10059.
- [141] F. Wangsell, P. Nordeman, J. Savmarker, R. Emanuelsson, K. Jansson, J. Lindberg, A. Rosenquist, B. Samuelsson, M. Larhed, Investigation of α -phenylnorstatine and α -benzylnorstatine as transition state isostere motifs in the search for new BACE-1 inhibitors, *Bioorg. Med. Chem.* 19 (2011) 145–155.

Hitesh V. Motwani received his Bachelor in Pharmaceutical Sciences (2003) from Mumbai University, India and M.Sc. in Drug Chemistry (2005) from Newcastle University, UK. A Ph.D. in Environmental Chemistry (2011) was obtained from Stockholm University, Sweden, under the supervision of Professor Margareta Törnqvist. Subsequently, two years of post-doctoral study in Medicinal Chemistry was done in Professor Mats Larhed's group at Uppsala University, Sweden. Hitesh is currently Researcher at the Dept. of Materials and Environmental Chemistry, Stockholm University. His research interest spans the disciplines of Organic- and Bioorganic Chemistry, Medicinal Chemistry and Chemical Toxicology. At present, the research is focused to investigate the interactions of electrophilically reactive compounds with biomolecules, e.g. DNA and hemoglobin, to understand the associated toxicological behavior.

Maria De Rosa received her *Laurea* in Chemistry and Pharmaceutical Technologies, at Sapienza University of Rome, Italy (2007). Her Ph.D. was obtained in 2012 from University of Siena, Italy, under the supervision of Professor Federico Corelli. Post-doctoral study in Medicinal Chemistry was carried out (2012–2013) in the group of Professor Mats Larhed, Uppsala University, Sweden. At present, Maria is Researcher at the Department of Cell and Molecular Biology, Uppsala University, Sweden. Her research interest spans the disciplines of Organic and Medicinal Chemistry focusing on design and synthesis of new anti-tuberculosis entities.

Luke R. Odell was born in Tamworth, Australia in 1981. He graduated with an Honours BSc. in Forensic Science from the University of Newcastle, Australia in 2002. He completed his PhD studies at the same university under the guidance of Professor Adam McCluskey in 2006 working on the synthesis of enzyme inhibitors. In 2006, he took up a postdoctoral position with Professor Mats Larhed at Uppsala University. Since 2011, he has been an Associate Professor at Uppsala University and research interests include microwave-assisted chemistry, heterocyclic chemistry, PET chemistry and medicinal chemistry.

Anders Hallberg received his PhD from Lund University in 1980. After a postdoctoral period at the University of Arizona he joined Astra in Lund where he was later appointed Director of the Department of a Medicinal Chemistry. In 1990, Anders Hallberg was appointed to the Chair in Medicinal Chemistry at Uppsala University. He was elected President of Uppsala University in 2006 and held that position to 2012. His research interests include peptidomimetics, protease inhibitors and the development of fast, robust and selective organic reactions.

Mats Larhed received his PhD in 1997 and became a full professor in 2007. He holds the position as Chair of the Division of Organic Pharmaceutical Chemistry and as Head of Preclinical PET at Uppsala University. Dr Larheds main research focus has been towards the development of fast and selective synthetic methods for use in preparative medicinal chemistry. His work in microwave-assisted metal-catalysis covers different types of palladium-catalyzed coupling reactions, gas-free carbonylations and the development of non-resonant continuous flow methodologies. During the last ten years he has been increasingly engaged in the development of enzyme inhibitors for potential treatment of HIV, Malaria, Alzheimers disease and tuberculosis.